Deep inelastic scattering on the deuteron in the Bethe-Salpeter formalism. II. Realistic *NN* interaction

A. Yu. Umnikov* and F. C. Khanna
University of Alberta, Edmonton, Alberta, Canada T6G 2J1
and TRIUMF, 4004 Wesbrook Mall, Vancouver, British Columbia, Canada V6T 2A3

L. P. Kaptari
Bogoliubov Laboratory of Theoretical Physics, Joint Institute for Nuclear Research, Dubna, Russia
(Received 28 August 1996)

We present a systematic study of the leading twist structure functions of the deuteron, F_2^D, $b_{1,2}^D$, and g_1^D in a fully relativistic approach. Our study is based on a realistic Bethe-Salpeter amplitude for the deuteron, which is obtained as a solution to the homogeneous Bethe-Salpeter equation with a realistic *NN* kernel. Particular effort is made to connect the structure functions to the densities of the appropriate charges and currents. This allows for a systematic comparison between relativistic and nonrelativistic calculations by analyzing the same densities in both approaches. Thus, the sources of the relativistic effects in the structure functions are understood and clearly distinguished from variations caused by the differences in the model parameters. We present both the formalism and extensive numerical calculations for all steps of our analysis. We find that the nonrelativistic and relativistic calculations are qualitatively very much alike. However, three main features systematically distinguish a consistent relativistic approach from the nonrelativistic one: (i) the binding effects are larger, (ii) the effect of Fermi motion at high x is stronger, and (iii) the relativistic description of the structure functions $b_{1,2}^D$ is fully consistent, unlike the nonrelativistic approach, which is internally inconsistent and violates the fundamental sum rules. [S0556-2813(97)02310-8]

PACS number(s): 25.30.−c, 13.60.Hb, 13.40.−f

I. INTRODUCTION

This paper is the second of two papers devoted to a study of deep inelastic lepton scattering (inclusive electroproduction) on the deuteron within the Bethe-Salpeter (BS) formalism. The first paper [1], presented a formal approach to deep inelastic scattering within the BS formalism. The emphasis of this work was on the self-consistency of the method, and the development of all aspects of the formalism such that it could be applied to a study of realistic cases of reactions. A basic analysis was performed utilizing the operator product expansion method in the leading twist approximation with the results given in the space of the moments of the structure functions. In principle, the structure functions (SF) can be recovered from the known moments by applying the inverse Mellin transform. Analysis of the lower moments of the deuteron structure function allowed us to establish a formal consistency in the approach and to prove important sum rules. However, only simple illustrative numerical estimates were performed in the ''scalar deuteron'' model, which itself is rather far from reality. It was stated that in order to complete the study the following tasks had to be done. First, explicit formulas for the deuteron spin-averaged and spin-dependent structure functions needed to be derived and, second, the structure functions had to be computed in a realistic meson-nucleon theory. The present paper deals with both these tasks.

Some of the preliminary results, including the solution of the BS equation with realistic *NN* interactions, have been discussed briefly [2–4]. Our calculations within the BS formalism for the deuteron are presented systematically and in detail for the first time in this paper. No calculations by other authors have ever been performed within the BS formalism with realistic amplitudes.

This paper does not contain a simple collection of results reported elsewhere, nor is it based solely on the direct application of the formalism developed in Ref. [1], but rather it presents a better understanding of the formal and physical aspects of the process. Indeed, any calculation of realistic structure functions depends on a realistic BS amplitude, which we have computed numerically using a Wick rotation [1,2]. The formalism of Ref. [1] then allows us to calculate the physical moments of the structure functions using the deuteron amplitude. However, the *numerical transform* from the moments to the structure functions (the inverse Mellin transform) is not a well-defined operation [2,3] and a new method had to be developed. In this context, we found it beneficial to use the formalism developed in Refs. [5–7] in the late 1970's (see also [8]). This formalism is more convenient if we deal with structure functions, rather than the moments of structure functions (although of course, it is mathematically equivalent). The new formalism allows for a numerical treatment of the ''inverse Wick rotation'' of the BS amplitude when applied to the calculation of the structure functions. Incorporation of this formalism into the calculation of the deuteron structure functions is another goal of the present paper.

In recent years a number of studies of deep inelastic scattering of leptons from the deuteron have been undertaken in which various manifestations of the relativistic features of

*On leave from INFN, Sezione di Perugia and Department of Physics, University of Perugia, via A. Pascoli, Perugia, I-06100, Italy.

the deuteron have been investigated [9–14]. These results certainly influenced our subsequent analysis since the first publication [1], and the corresponding development of the formalism is considered in this paper as well.

Another new and distinguishing feature of the present paper is the special accent on the systematic comparison of the relativistic and nonrelativistic approaches. To do this, we consider the connection of the structure functions to the densities of appropriate charges and currents, and then analyze these densities in both relativistic and nonrelativistic approaches. In this way, we are able to trace the origin of the relativistic effects and to demonstrate inconsistencies in the nonrelativistic approximations. The paper contains a number of illustrations at every step of our analysis.

Finally, results for the structure functions published previously [2,3] have been recalculated using the new method resulting in some corrections, albeit small, to the SF.

The paper is organized as follows. In Sec. II, we define the densities of the currents which are used later in the analysis of the deep inelastic scattering. For this purpose, the realistic BS amplitude of the deuteron is presented, and the relativistic and nonrelativistic expressions for densities are defined and calculated within realistic models. In Sec. III the relativistic formalism of our approach to the deep inelastic scattering on the deuteron is developed which includes explicit relativistic and nonrelativistic formulas for the structure functions, and the sum rules for the structure functions are analyzed. Section IV contains results of both relativistic and nonrelativistic calculations of the structure functions F_2^D, $b_{1,2}^D$, and g_1^D in realistic models. In Sec. V the summary of results of the paper is presented. Two Appendixes contain important technical details.

II. ANATOMY OF THE DEUTERON

A. Realistic *NN* interaction and Bethe-Salpeter amplitude

The basis of our approach to the relativistic description of deep inelastic scattering from the deuteron is a nucleon-nucleon BS amplitude. The general self-consistency of such an approach has been analyzed in our previous paper [1]. The way to construct relevant matrix elements has been presented and important sum rules have been proved, both without reference to any particular model for the BS amplitude. A naive numerical estimate has been completed within the *scalar deuteron* model which is found to be in qualitative agreement with the nonrelativistic theory of deep inelastic scattering [15–17].

Yet, for realistic calculations of the deuteron structure functions we need a *realistic* BS amplitude, which provides us with a good description of the bulk of the deuteron properties. This is the same ideology as is used in constructing the realistic wave function of the deuteron [18–22]. The most consistent way to obtain a realistic BS amplitude is to solve the dynamical problem with a *realistic model* of the *NN* interaction. However, the realistic *NN* interaction still cannot be derived explicitly from the underlying fundamental theory, QCD, nor from nonrelativistic approximations, such as chiral perturbation theory, although some progress has been achieved in recent years [23,24]. Alternatively, the parameters of the *NN* interaction can be fixed in the traditional manner from the available experimental data on nucleon-nucleon scattering (phase shifts analysis), if the general form of interaction is somehow determined [18,19,22,25]. Unfortunately, the parametrization of the *NN* interaction is dependent on the choice of a dynamical equation. In spite of a definite similarity of the sets of parameters in all realistic models there is no universal form for all nonrelativistic and relativistic potentials.

The only one parametrization of the *NN* interaction available for the BS equation, is that of Fleischer and Tjon [25]. It probably needs revision [26], by incorporating new data on the nucleon-nucleon phase shift analysis [27]. However, this parametrization has been used as the basis for our recent calculation of the BS amplitude of the deuteron [2]. The meson parameters (masses, coupling constants, cutoff parameters) have been taken to be the same as in Refs. [25,21], except for the coupling constant of the scalar σ meson, which has been adjusted to provide a numerical solution of the homogeneous BS equation, and a few other minor adjustments, in view of the following considerations. First, we used a simplified form of the propagator of the vector mesons, omitting the $k_\mu k_\nu/\mu_B^2$ term. Second, a different numerical procedure to solve the eigenvalue problem for the BS equation can also affect the value of parameters.

The detailed formalism preceding the numerical solution of the BS equation for the deuteron is presented in Ref. [1]. The Fredholm system of ''Wick rotated'' equations with all meson exchanges is solved by an iteration procedure with two-dimensional Gaussian integration (see, e.g., Ref. [28]). The following eight components of the BS amplitude of the deuteron:

$$\psi_{p1},\psi_{a1}^0,\psi_{v1},\psi_{a0},\psi_{a2},\psi_{t1}^0,\psi_{t0},\psi_{t2}, \tag{2.1}$$

have been computed as scalar functions of two variables p_0 and $|\boldsymbol{p}|$, components of the momentum four-vector. An analytic parametrization of these components is now available [29].

Since the one-boson exchange potential [21,25] was used only with a minor adjustment, our present solution does not contain any new or different physics. This also strongly suggests that the BS amplitudes are indeed realistic, and provide a good description of *NN* scattering, static properties, and form factors of the deuteron [21,22,25,30–33]. All parameters are presented in Table I. The set of parameters includes the nucleon mass m, the deuteron binding energy ε_D, and, therefore, the deuteron mass $M_D=2m+\varepsilon_D$. The coupling constants are given in accordance with our definition of the meson-nucleon form factors

$$F_B(k)=\frac{\Lambda^2-\mu_B^2}{\Lambda^2-k^2}, \tag{2.2}$$

where Λ is a cutoff parameter (see Table I).

B. Static properties and densities

In order to compare different models of the deuteron and define to what degree each of the models is *realistic*, it is natural to calculate various observables within these models and compare them with each other and with the experimental data. The canonical way to do this is to calculate the nucleon

TABLE I. The set of parameters of the kernel of BS equation used in this work.

meson B	coupling constants $g_B^2/(4\pi)$;$[g_v/g_t]$	mass μ_B, GeV	cutoff Λ,GeV	isospin
σ	12.2	0.571	1.29	0
δ	1.6	0.961	1.29	1
π	14.5	0.139	1.29	1
η	4.5	0.549	1.29	0
ω	27.0; [0]	0.783	1.29	0
ρ	1.0; [6]	0.764	1.29	1

$m=0.939$ GeV, $\varepsilon_D=-2.225$ MeV

contributions to static observables, for example, the mean square radius, magnetic, and quadrupole moments [18–22,30]. The mesonic corrections are quite small and depend upon additional model assumptions. Most of the modern realistic models give a quite good description of the static properties or provide a plausible explanation in the case of a minor discrepancy. The reaction observables such as form factors and structure functions, are more model dependent. These differences are often used as a tool for discriminating between models or various calculational techniques using the models.

A direct comparison of the wave functions and amplitudes usually seems to be less meaningful. Still, in many cases particular properties of the wave functions and amplitudes directly indicate what will happen when observables are calculated. A prime example is the D-wave admixture, which directly affects values of the magnetic and quadrupole moments, the tensor analyzing power T_{20}, and the spin-dependent structure functions of the deuteron g_1^D and b_2^D. Another example, the high momentum ''tail'' of the wave function (amplitude) dominates in the observables for some kinematic conditions with a high momentum transfer. However, the interpretation and properties of BS amplitudes are very different from those of the wave functions; a direct comparison between them is impossible.

Recently, it has been argued that new intuition can be developed in working with the BS amplitude [30,29] by considering the charge and current densities and comparing them to similar calculations using the nonrelativistic approach with wave functions. The charge and current densities are more directly linked to the observables than wave functions and amplitudes. Following this idea, we calculate the charge and current densities which are related to the various structure functions in deep inelastic scattering.

In many important cases the nucleon contribution to the deuteron observable $\langle\mathcal{O}\rangle$ is defined by the triangle diagram (see Fig. 1)

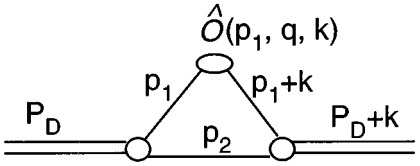

FIG. 1. Triangle graph for nucleon contribution to the deuteron matrix element of operator $\hat{\mathcal{O}}$.

$$\langle\mathcal{O}\rangle_M = i\int\frac{d^4p}{(2\pi)^4}\mathrm{Tr}\{\overline{\Psi}_M(p_0,\boldsymbol{p})\hat{\mathcal{O}}(p_1,q,k)\Psi_M \times(p_0+k_0,\boldsymbol{p}+\boldsymbol{k})(\hat{p}_2-m)\}, \tag{2.3}$$

where $p_{1,2}=P_D/2\pm p=(M_D/2\pm p_0,\pm\boldsymbol{p})$, $P_D=(M_D,\boldsymbol{0})$ is the deuteron momentum in the rest frame, $p=(p_0,\boldsymbol{p})$ is the relative momentum of the nucleons, $\hat{\mathcal{O}}(p_1,q,k)$ is an appropriate operator, and $\Psi_M(p_0,\boldsymbol{p})$ is the BS amplitude for the deuteron with M being the deuteron's total angular momentum projection (see Ref. [1] for definition and conventions for $\Psi_M(p_0,\boldsymbol{p})$). The operator $\hat{\mathcal{O}}(p_1,q,k)$ is written in a general form, which depends on nucleon momentum, p_1 and two external momenta q and k. q does not appear in the lower part of the diagram and k adds to the nucleon momentum. In the present paper we consider only the case with $k=0$.

The explicit form of the operators and the structure of the deuteron matrix elements relevant to deep inelastic scattering have been studied previously by several authors [16,17,9–11,1]. One such method of finding a form of the operator for deep inelastic scattering is that of Wilson's operator product expansion [34] applied within an effective meson nucleon theory [16,17,35,1]. Another possible approach is based on a parametrization of the operators in the most general form with phenomenological analysis or interpretation within models for quark-nucleon amplitudes [9–11,8,36]. Both approaches lead to the same results in the ''convolution approximation'' which assumes that the deformation of the nucleon operator off-mass-shell can be neglected. In the present paper we do not concentrate on the differences between these two approaches; that is, our analysis does not go beyond the convolution approximation.

The vector γ_μ, and the axial vector $\gamma_5\gamma_\mu$ operators are relevant here. The matrix elements of the selected components of these operators are given by

$$\begin{Bmatrix}\langle\gamma_0\rangle_M\\ \langle\gamma_3\rangle_M\\ \langle\gamma_5\gamma_0\rangle_M\\ \langle\gamma_5\gamma_3\rangle_M\end{Bmatrix} = \frac{i}{2M_D}\int\frac{d^4p}{(2\pi)^4}\mathrm{Tr}\left\{\overline{\Psi}_M(p_0,\boldsymbol{p})\begin{Bmatrix}\gamma_0\\ \gamma_3\\ \gamma_5\gamma_0\\ \gamma_5\gamma_3\end{Bmatrix} \times\Psi_M(p_0,\boldsymbol{p})(\hat{p}_2-m)\right\}. \tag{2.4}$$

Three main combinations of these matrix elements are im-

portant for deep inelastic scattering. They are presented below along with the corresponding deuteron structure functions:

$$F_2^D \to \frac{1}{3}\sum_M \{\langle\gamma_0\rangle_M + \langle\gamma_3\rangle_M\}, \tag{2.5}$$

$$b_2^D \to \{\langle\gamma_0\rangle_{M=1} + \langle\gamma_3\rangle_{M=1}\} - \{\langle\gamma_0\rangle_{M=0} + \langle\gamma_3\rangle_{M=0}\}, \tag{2.6}$$

$$g_1^D \to \{\langle\gamma_5\gamma_0\rangle_{M=1} + \langle\gamma_5\gamma_3\rangle_{M=1}\}, \tag{2.7}$$

where $\to$ means ''corresponding to'' and does not have a direct mathematical interpretation. Explicit connection of these matrix elements to the structure functions will be discussed in Sec. III. These matrix elements represent charges and currents, vector and axial vector, calculated for deuteron states with different combinations of total angular momentum projection M. Properties of these matrix elements, including rigorous sum rules for the charges, are later used to discuss the structure functions.

Let us start from the matrix elements involved in Eq. (2.5). The first term $\langle\gamma_0\rangle_M$ is the charge of the conserved vector current and, since it is independent of M, the following sum rules can be immediately written down (see, e.g., [16,1]):

$$\frac{1}{3}\sum_M \langle\gamma_0\rangle_M = \langle\gamma_0\rangle_M = 1. \tag{2.8}$$

Obviously this sum rule is also valid in the nonrelativistic approaches since it is just a normalization condition for both the wave functions and BS amplitudes. To make more meaningful use of this matrix element and compare our approach to other realistic approaches, we define the charge density in the BS formalism as (see Appendix A for the explicit form)

$$\langle\gamma_0\rangle^{\rm BS}(\boldsymbol{p}) = \frac{i}{12\pi^2 M_D}\sum_M \int \frac{dp_0}{2\pi} \times {\rm Tr}\{\overline{\Psi}_M(p_0,\boldsymbol{p})\gamma_0\Psi_M(p_0,\boldsymbol{p})(\hat{p}_2 - m)\}, \tag{2.9}$$

$$\frac{1}{4\pi}\int d\boldsymbol{p}\langle\gamma_0\rangle^{\rm BS}(\boldsymbol{p}) = 1. \tag{2.10}$$

In the nonrelativistic limit this corresponds to the momentum density [17,1,12]

$$\langle\gamma_0\rangle^{\rm NR}(\boldsymbol{p}) = \frac{1}{6\pi^2}\sum_M |\Psi_M(\boldsymbol{p})|^2 = [u^2(|\boldsymbol{p}|) + w^2(|\boldsymbol{p}|)], \tag{2.11}$$

$$\frac{1}{4\pi}\int d\boldsymbol{p}\langle\gamma_0\rangle^{\rm NR}(\boldsymbol{p}) = 1, \tag{2.12}$$

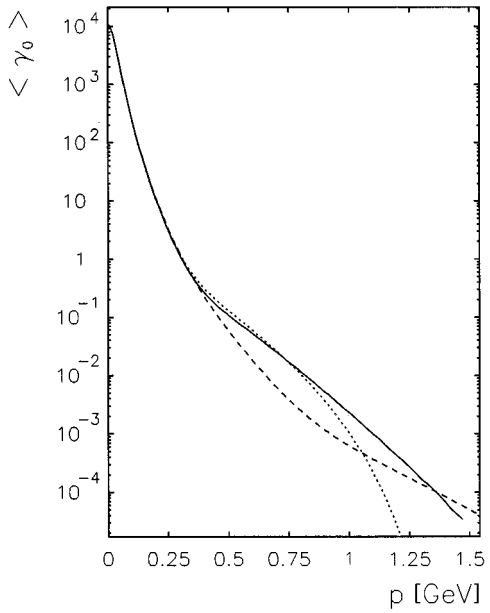

FIG. 2. The charge density in the deuteron, Eqs. (2.9) and (2.11), calculated in different models, nonrelativistic and relativistic, the Bethe-Salpeter amplitude (solid), the Bonn wave function (dashed), and the Paris wave function (dotted).

where $\Psi_M(\boldsymbol{p})$ is a nonrelativistic wave function of the deuteron with u and w being its S- and D-wave components. The densities $\langle\gamma_0\rangle(\boldsymbol{p})$, calculated in three realistic models [18,19,2], are shown in Fig. 2. Certain model differences at $|\boldsymbol{p}| > 0.5$ GeV are present, however there is no distinguishing feature of the relativistic density.

Similarly, we consider other components of the vector and axial matrix elements. The relativistic densities $\langle\gamma_3\rangle^{\rm BS}(\boldsymbol{p})$, $\langle\gamma_5\gamma_0\rangle^{\rm BS}(\boldsymbol{p})$, are defined by replacing γ_0 with γ_3, $\gamma_5\gamma_0$, and taking appropriate combination of the matrix elements with different M in Eq. (2.9). The explicit expressions for all densities in terms of the components of the BS amplitude are presented in the Appendix A.

The nonrelativistic densities are calculated from a nonrelativistic reduction [17,1,12]. Here we present the most interesting densities of them. A remarkable feature of the nonrelativistic densities is that they have the same angular dependences as the corresponding relativistic densities.

The third spatial component of the vector current in the nonrelativistic limit is

$$\langle\gamma_3\rangle^{\rm NR}(\boldsymbol{p}) = \frac{p_3}{6\pi^2 m}\sum_M |\Psi_M(\boldsymbol{p})|^2 + \mathcal{O}\left(\frac{|\boldsymbol{p}|^3}{m^3}\right) \simeq \frac{|\boldsymbol{p}|\cos\vartheta}{m}[u^2(|\boldsymbol{p}|) + w^2(|\boldsymbol{p}|)], \tag{2.13}$$

where ϑ is polar angle of vector $\boldsymbol{p}$. Note that this density has a suppression factor of $\sim|\boldsymbol{p}|/m$, due to a mixing of the upper and lower components of the Dirac spinors by nondiagonal matrix γ_3. Since the angular dependence of the explicit form of the relativistic density $\langle\gamma_3\rangle^{\rm BS}(\boldsymbol{p})$ is also absorbed in the factor $\cos\vartheta$ (see Appendix A), the integrals of both the relativistic and nonrelativistic densities $\langle\gamma_3\rangle$ over $d\boldsymbol{p}$ are zero:

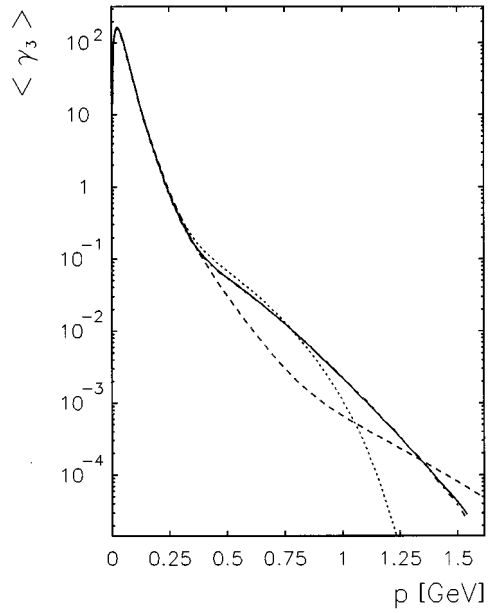

FIG. 3. The $\langle \gamma_3 \rangle(\boldsymbol{p})$ in the deuteron calculated in different models: BS amplitude (solid), the Bonn wave function (dashed), and the Paris wave function (dotted).

$$\int d\boldsymbol{p}\langle \gamma_3 \rangle^{\mathrm{BS}}(\boldsymbol{p}) = \int d\boldsymbol{p}\langle \gamma_3 \rangle^{\mathrm{NR}}(\boldsymbol{p}) = \langle \gamma_3 \rangle \propto \int_{-1}^{1} d(\cos\vartheta)\cos\vartheta = 0. \tag{2.14}$$

These densities for realistic models are shown in Fig. 3 with $\theta = 0$. Basically, they just reflect the behavior of the charge densities from Fig. 2 in accordance with the nonrelativistic formula (2.13). For illustration, the curve representing the BS density from Fig. 2 multiplied by the factor $|\boldsymbol{p}|/m$ is also shown (dash-dotted). Surprisingly enough, it can barely be distinguished from the exact $\langle \gamma_3 \rangle^{\mathrm{BS}}(\boldsymbol{p})$ (solid line) even at momenta higher than m.

Two examples of spin-dependent densities are

$$\langle \gamma_0 \rangle^{\mathrm{NR}}_{M=1}(\boldsymbol{p}) - \langle \gamma_0 \rangle^{\mathrm{NR}}_{M=0}(\boldsymbol{p}) \simeq -\frac{3}{2} P_2(\cos\vartheta) w(|\boldsymbol{p}|) \times [2\sqrt{2}u(|\boldsymbol{p}|) + w(|\boldsymbol{p}|)], \tag{2.15}$$

$$\langle \gamma_5\gamma_3 \rangle^{\mathrm{NR}}_{M=1}(\boldsymbol{p}) \simeq u^2(|\boldsymbol{p}|) - \frac{1}{2} w^2(|\boldsymbol{p}|) + P_2(\cos\vartheta) w(|\boldsymbol{p}|) \times [w(|\boldsymbol{p}|) - \sqrt{2}u(|\boldsymbol{p}|)], \tag{2.16}$$

where $P_2(x)$ is the Legendre polynomial. We also can easily write down sum rules for the spin-dependent densities (2.15) and (2.16)

$$\int d\boldsymbol{p}\{\langle \gamma_0 \rangle^{\mathrm{NR}}_{M=1}(\boldsymbol{p}) - \langle \gamma_0 \rangle^{\mathrm{NR}}_{M=0}(\boldsymbol{p})\} \propto \int_{-1}^{1} d(\cos\vartheta) P_2(\cos\vartheta) = 0, \tag{2.17}$$

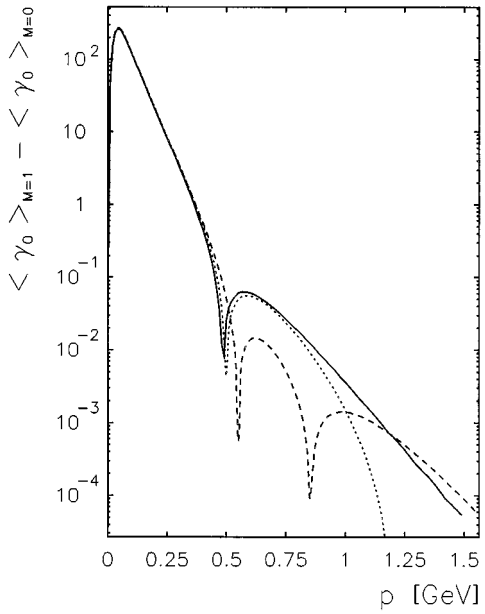

FIG. 4. The ''tensor density'' of the deuteron, $\langle \gamma_0 \rangle^{\mathrm{NR}}_{M=1}(\boldsymbol{p}) - \langle \gamma_0 \rangle^{\mathrm{NR}}_{M=0}(\boldsymbol{p})$, calculated in different models. To exclude the angular dependence the densities are divided by $P_2(\cos\theta)$: BS amplitude (solid), the Bonn wave function (dashed), and the Paris wave function (dotted).

$$\frac{1}{4\pi}\int d\boldsymbol{p}\langle \gamma_5\gamma_3 \rangle^{\mathrm{NR}}(\boldsymbol{p}) = 1 - \frac{3}{2} w_D, \tag{2.18}$$

where w_D is the weight of the D wave in the deuteron. The relativistic analog of the sum rule (2.18) can be used for an estimate of the ''admixture'' of the D wave in the relativistic formalism, which otherwise does not allow for probabilistic interpretation. Numerically we have

$$\frac{1}{4\pi}\int d\boldsymbol{p}\langle \gamma_5\gamma_3 \rangle^{\mathrm{BS}}(\boldsymbol{p}) \simeq 0.9215, \tag{2.19}$$

which gives us an estimate of $w_D \approx 5\%$.[1]

The realistic model densities (2.15) and (2.16) are presented in Figs. 4 and 5, respectively. These two examples confirm the conclusions of the previous illustrations: (i) realistic models are in a reasonable agreement with one another, providing a good description of the charge and current densities of the deuteron, and (ii) in spite of some model variations at high momentum, there is no distinguishing feature of the densities obtained in a relativistic BS formalism. Therefore, we cannot expect relativistic effects due to the *form* of the densities to be significant. However, this conclusion does not preclude the possibility of observable effects generated by the differences in the relativistic and nonrelativistic description of the deep inelastic reaction.

[1]There can be corrections, $\mathcal{O}(|\boldsymbol{p}|^2/m^2)$, to the density $\langle \gamma_5\gamma_3 \rangle^{\mathrm{NR}}_{M=1}(\boldsymbol{p})$, see Refs. [35,12]. However, their estimated contribution to integral (2.18) is small, $\lesssim 1\%$.

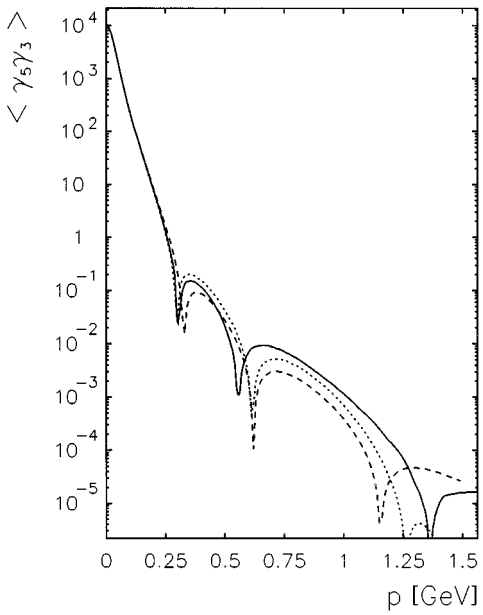

FIG. 5. The spin density $\langle \gamma_5 \gamma_3 \rangle_{M=1}(\boldsymbol{p})$ in the deuteron calculated in different models (see Sec. II B for definitions). To exclude the angular dependence for the present figure, densities are integrated over all angles: BS amplitude (solid), the Bonn wave function (dashed), and the Paris wave function (dotted).

III. RELATIVISTIC THEORY OF DEEP INELASTIC SCATTERING ON THE DEUTERON

A. Definitions and kinematics

We start with the general form of the hadronic tensor of the deuteron with the total angular momentum projection M, keeping only the leading twist structure functions

$$
\begin{aligned}
&W^D_{\mu\nu}(q,P_D,M) \\
&\quad=\left(-g_{\mu\nu}+\frac{q_\mu q_\nu}{q^2}\right)F_1^D(x_D,Q^2,M)+\left(P_{D\mu}-q_\mu\frac{P_Dq}{q^2}\right) \\
&\quad\times\left(P_{D\nu}-q_\nu\frac{P_Dq}{q^2}\right)\frac{F_2^D(x_D,Q^2,M)}{P_Dq} \\
&\quad+\frac{iM_D}{P_Dq}\epsilon_{\mu\nu\alpha\beta}q^\alpha S_D^\beta(M)g_1^D(x_D,Q^2),
\end{aligned}
\tag{3.1}
$$

where $q=(\nu,0,0,-\sqrt{\nu^2+Q^2})$ is the momentum transfer, $Q^2=-q^2$, $x_D=Q^2/(2P_Dq)$ [in the rest frame of the deuteron $x_D=Q^2/(2M_D\nu)$], $S_D(M)$ is the deuteron spin (see Appendix B), and $F_{1,2}^D$ and g_1^D are deuteron structure functions (SF's). Averaged over M, this expression leads to the well-known form of the spin-independent hadronic tensor which is valid for hadrons with any spin:

$$
W^D_{\mu\nu}(q,P_D)=\frac{1}{3}\sum_M W^D_{\mu\nu}(q,P_D,M)
$$

$$
\begin{aligned}
&=\left(-g_{\mu\nu}+\frac{q_\mu q_\nu}{q^2}\right)F_1^D(x_D,Q^2) \\
&\quad+\left(P_{D\mu}-q_\mu\frac{P_Dq}{q^2}\right)\left(P_{D\nu}-q_\nu\frac{P_Dq}{q^2}\right) \\
&\quad\times\frac{F_2^D(x_D,Q^2)}{P_Dq},
\end{aligned}
\tag{3.3}
$$

where $F_{1,2}^D(x_D,Q^2)$ are the result of averaging $F_{1,2}^D(x_D,Q^2,M)$. Other structure functions can be obtained from other combinations of $W^D_{\mu\nu}(q,P_D,M)$ with different M:

$$
W^D_{\mu\nu}(q,P_D,M=1)-W^D_{\mu\nu}(q,P_D,M=-1)\propto g_1^D(x_D,Q^2),
\tag{3.4}
$$

$$
W^D_{\mu\nu}(q,P_D,M=1)-W^D_{\mu\nu}(q,P_D,M=0)\propto b_{1,2}^D(x_D,Q^2).
\tag{3.5}
$$

The Eqs. (3.2), (3.4), and (3.5) are the basis for the experimental measurements of the deuteron SF's. However, for theoretical studies of the hadronic tensor and SF's, the projection technique is more convenient. All relevant formulas for the projection technique are presented in Appendix B while background information on the SF $b_{1,2}^D$ can be found in Refs. [37–40].

To calculate the hadronic tensor of the deuteron we follow the general formalism of our approach

$$
\begin{aligned}
W^D_{\mu\nu}(q,P_D,M)=i\int\frac{d^4p}{(2\pi)^4}\mathrm{Tr}\{&\overline{\Psi}_M(p_0,\boldsymbol{p}) \\
&\times\hat{W}^N_{\mu\nu}(p_1,q)\Psi_M(p_0,\boldsymbol{p})(\hat{p}_2-m)\}.
\end{aligned}
\tag{3.6}
$$

The nucleon tensor operator $\hat{W}^N_{\mu\nu}(q,p)$ has been studied extensively in recent years [16,35,1,9,10,12,8] and we use a well-established form of the operator, leading to the convolution formula [41]

$$
\hat{W}^N_{\mu\nu}(q,p)=\hat{W}_{\{\mu\nu\}}(q,p)+\hat{W}_{[\mu\nu]}(q,p),
\tag{3.7}
$$

$$
\hat{W}_{\{\mu\nu\}}(q,p)=\frac{\hat{q}}{2pq}W^N_{\mu\nu}(q,p),
\tag{3.8}
$$

$$
\hat{W}_{[\mu\nu]}(q,p)=\frac{i}{2pq}\epsilon_{\mu\nu\alpha\beta}q^\alpha\gamma^\beta\gamma_5 g_1^N(q,p),
\tag{3.9}
$$

where $\{\cdots\}$ and $[\cdots]$ denote symmetrization and antisymmetrization of indices, and $g_1^N(q,p)=g_1^N(x,Q^2)$ is the spin-dependent nucleon SF. The hadronic tensor of the nucleon $W_{\mu\nu}(p,q)^N$ is defined as

$$W^N_{\mu\nu}(q,p)=\left(-g_{\mu\nu}+\frac{q_\mu q_\nu}{q^2}\right)F_1^N(x,Q^2)+\left(p_\mu-q_\mu\frac{pq}{q^2}\right)\times\left(p_\nu-q_\nu\frac{pq}{q^2}\right)\frac{F_2^N(x,Q^2)}{pq},\tag{3.10}$$

where $x=Q^2/(2pq)$ and $F^N_{1,2}$ are the nucleon SF's. The small effects of the off-mass-shell deformation of the nucleon tensor [9,12,42] are not considered here, since these effects do not affect sum rules for the SF and do not noticeably change the absolute values of the SF's. It is for this reason that the SF's $F^N_{1,2}$ in Eq. (3.10) do not depend on p^2, but only on q^2 and pq.

Using the projectors (see Appendix B), we extract SF's from the hadronic tensor of the deuteron:

$$F_1^D(x_N,Q^2,M)=i\int\frac{d^4p}{(2\pi)^4}F_1^N\left(\frac{x_Nm}{p_{10}+p_{13}},Q^2\right)\frac{\mathrm{Tr}\{\overline{\Psi}_M(p_0,\boldsymbol{p})(\gamma_0+\gamma_3)\Psi_M(p_0,\boldsymbol{p})(\hat{p}_2-m)\}}{2(p_{10}+p_{13})},\tag{3.11}$$

$$F_2^D(x_N,Q^2,M)=i\int\frac{d^4p}{(2\pi)^4}F_2^N\left(\frac{x_Nm}{p_{10}+p_{13}},Q^2\right)\frac{\mathrm{Tr}\{\overline{\Psi}_M(p_0,\boldsymbol{p})(\gamma_0+\gamma_3)\Psi_M(p_0,\boldsymbol{p})(\hat{p}_2-m)\}}{2M_D},\tag{3.12}$$

$$g_1^D(x_N,Q^2)=i\int\frac{d^4p}{(2\pi)^4}g_1^N\left(\frac{x_Nm}{p_{10}+p_{13}},Q^2\right)\frac{\mathrm{Tr}\{\overline{\Psi}_M(p_0,\boldsymbol{p})(\gamma_0+\gamma_3)\gamma_5\Psi_M(p_0,\boldsymbol{p})(\hat{p}_2-m)\}|_{M=1}}{2(p_{10}+p_{13})},\tag{3.13}$$

where $x_N=Q^2/(2m\nu)$ is the Bjorken scaling variable,[2] i.e., this is x for the on-mass-shell nucleon at rest, p_{10} and p_{13} are the time and third components of the struck nucleon momentum. Formulas (3.11) and (3.12) have not been averaged over the projection M, since the present form helps in understanding the SF $b^D_{1,2}$. For instance Eq. (3.12) gives two independent ''SF's,'' with $M=\pm1$ and $M=0$, which are related to the usual spin-independent SF F_2^D and a new SF b_2^D:

$$F_2^D(x_N,Q^2)=\frac{1}{3}\sum_{M=0,\pm1}F_2^D(x_N,Q^2,M),\tag{3.14}$$

$$b_2(x_N,Q^2)=F_2^D(x,Q^2,M=+1)-F_2^D(x,Q^2,M=0),\tag{3.15}$$

$$F_2^D(x_N,Q^2,M=+1)=F_2^D(x_N,Q^2,M=-1).\tag{3.16}$$

Note, the SF $F_2^D(x,Q^2,M)$ is independent of the lepton polarization, therefore both SF's F_2^D and b_2^D can be measured in experiments with an unpolarized lepton beam and polarized deuteron target. In view of Eq. (3.16), only one of the SF's $[F_2^D(x,Q^2,M)]$ is needed, in addition to the spin-independent $F_2^D(x,Q^2)$, in order to obtain $b_2(x,Q^2)$. The other SF b_1^D is related to the deuteron SF F_1^D the same way that b_2^D is related to F_2^D, viz. via Eq. (3.14) and $b_2^D=2xb_1^D$.

B. Singularities of the triangle diagram and calculation of structure functions

It has been shown previously [5–8] how the singular structure of the triangle graph (Fig. 1) rules the behavior of the spin-independent SF F_2^D. In particular, it is found that the relativistic impulse approximation satisfies unitarity conditions and provides the correct kinematical region of the variable x_N. However, for the exact covariant amplitude both these properties are violated in practical calculations when nonrelativistic wave functions of the deuteron are used. In this case one can argue that this introduces small deviations, which are not important for phenomenology. On the other hand, a realistic BS amplitude of the deuteron serves ideally for a consistent phenomenological application of the covariant theory of processes on the bound nucleons.

In order to calculate the SF's, given by Eqs. (3.12)–(3.15) and analyze the sum rules, the singularities of the triangle diagram should be explicitly taken into account. To do that, Eq. (3.12) is rewritten as

$$F_2^D(x_N,Q^2,M)=\frac{i}{2M_D}\int\frac{d^4p}{(2\pi)^4}F_2^N\left(\frac{x_Nm}{p_{10}+p_{13}},Q^2\right)\frac{1}{(p_1^2-m^2+i\epsilon)^2(p_2^2-m^2+i\epsilon)}\times\mathrm{Tr}\{\overline{\phi_M}(p_0,\boldsymbol{p})(\hat{p}_1+m)(\gamma_0+\gamma_3)(\hat{p}_1+m)\phi_M(p_0,\boldsymbol{p})(\hat{p}_2+m)\},\tag{3.17}$$

where $\phi_M(p_0,\boldsymbol{p})=(\hat{p}_1-m)\Psi_M(p_0,\boldsymbol{p})(\hat{p}_2-m)$ is the BS vertex function of the deuteron.

[2]Note that the ''native'' deuteron variable is $x_D=(m/M_D)x_N$, however, x_N is used more often.

Analysis of singularities in the complex p plane allows for one analytical integration in Eq. (3.17) [7]. After translation into variables which are used in the present paper, this integration is equivalent to picking the residue of the second nucleon pole, $p_{20}=\omega=\sqrt{m^2+\boldsymbol{p}^2}$ or $p_0=M_D/2-\omega$, in the complex p_0 plane when both of the following conditions are satisfied:

$$0<\omega-p_3<M_D\,. \tag{3.18}$$

The contribution to the integral (3.17), of the region of p beyond Eq. (3.18), is zero, i.e., different poles cancel each other. Note, that $p_{10}=M_D-\omega$ in the required pole. Calculating the residue in Eq. (3.17), one gets

$$F_2^D(x_N,Q^2,M)=\frac{1}{2M_D}\int\frac{d^3\boldsymbol{p}}{(2\pi)^3}F_2^N\left(\frac{x_N m}{M_D-\omega+p_3},Q^2\right)\Theta(M_D-\omega+p_3)\frac{1}{2\omega M_D^2(M_D-2\omega)^2}$$
$$\times\mathrm{Tr}\{\overline{\phi_M}(p_0,\boldsymbol{p})(\hat{p}_1+m)(\gamma_0+\gamma_3)(\hat{p}_1+m)\phi_M(p_0,\boldsymbol{p})(\hat{p}_2+m)\}_{p_0=M_D/2-\omega}, \tag{3.19}$$

where the Θ function guarantees the upper inequality condition (3.18) is satisfied, while the lower condition is always satisfied. It is instructive to note that the initial expression (3.6) contained both the spectator nucleon singularity and the singularities of the propagators of the struck nucleon. However, an accurate calculation of the integral shows that the physical SF of the deuteron has a correct kinematic limits in x, $0\leqslant x\leqslant M_D/m$, and is defined only by the spectator's pole $p_0=M_D/2-\omega$. This is an explicit illustration of the ''support'' property (see discussion in [41,8]).

It is useful to rewrite (3.19) in the convolution form

$$F_2^D(x_N,Q^2,M)=\int_{x_N}^{M_D/m}dy F_2^N\left(\frac{x_N}{y},Q^2\right)f_M^{N/D}(y), \tag{3.20}$$

where ''the effective distribution'' of nucleons in the deuteron is defined by

$$f_M^{N/D}(y)=\frac{1}{2M_D}\int\frac{d^3\boldsymbol{p}}{(2\pi)^3}\delta\left(y-\frac{M_D-w+p_3}{m}\right)\Theta(y)\frac{1}{2\omega M_D^2(M_D-2\omega)^2}$$
$$\times\mathrm{Tr}\{\overline{\phi_M}(p_0,\boldsymbol{p})(\hat{p}_1+m)(\gamma_0+\gamma_3)(\hat{p}_1+m)\phi_M(p_0,\boldsymbol{p})(\hat{p}_2+m)\}_{p_0=M_D/2-\omega}\,. \tag{3.21}$$

The SF's $F_{1,2}^D$ and $b_{1,2}^D$ are now calculated from

$$\begin{Bmatrix}F_1^D(x_N,Q^2)\\ b_1^D(x_N,Q^2)\end{Bmatrix}=\int_{x_N}^{M_D/m}\frac{dy}{y}\begin{Bmatrix}f^{N/D}(y)\\ \Delta f^{N/D}(y)\end{Bmatrix}F_1^N\left(\frac{x_N}{y},Q^2\right), \tag{3.22}$$

$$\begin{Bmatrix}F_2^D(x_N,Q^2)\\ b_2^D(x_N,Q^2)\end{Bmatrix}=\int_{x_N}^{M_D/m}dy\begin{Bmatrix}f^{N/D}(y)\\ \Delta f^{N/D}(y)\end{Bmatrix}F_2^N\left(\frac{x_N}{y},Q^2\right), \tag{3.23}$$

where the distributions $f^{N/D}$ and $\Delta f^{N/D}$ are given by

$$f^{N/D}(y)=\frac{1}{3}\sum_M f_M^{N/D}(y), \tag{3.24}$$

$$\Delta f^{N/D}(y)=f_1^{N/D}(y)-f_0^{N/D}(y). \tag{3.25}$$

Similarly, for the SF g_1^D we get

$$g_1^D(x_N,Q^2)=\int_{x_N}^{M_D/m}\frac{dy}{y}g_1^N\left(\frac{x_N}{y},Q^2\right)\vec{f}^{N/D}(y), \tag{3.26}$$

where the effective polarized distribution of nucleons in the deuteron is defined by

$$\vec{f}^{N/D}(y)=\frac{1}{2M_D}\int\frac{d^3\boldsymbol{p}}{(2\pi)^3}\delta\left(y-\frac{M_D-w+p_3}{m}\right)\Theta(y)\frac{1}{2\omega M_D^2(M_D-2\omega)^2}$$
$$\times\mathrm{Tr}\{\overline{\phi_{M=1}}(p_0,\boldsymbol{p})(\hat{p}_1+m)(\gamma_0+\gamma_3)\gamma_5(\hat{p}_1+m)\phi_{M=1}(p_0,\boldsymbol{p})(\hat{p}_2+m)\}_{p_0=M_D/2-\omega}\,. \tag{3.27}$$

C. Sum rules for the deuteron structure functions

Two sum rules can be written for the effective distribution $f_M^{N/D}(y)$:

$$\int_0^{M_D/m} f_M^{N/D}(y)dy = \frac{1}{4\pi}\int d\boldsymbol{p}\langle\gamma_0\rangle_M(\boldsymbol{p}) = \langle\gamma_0\rangle_M = 1, \tag{3.28}$$

$$\int_0^{M_D/m} y f_M^{N/D}(y)dy = \langle D|(\Theta_N)_\mu^\mu|D\rangle_M = 1-\delta_N, \tag{3.29}$$

where $(\Theta_N)_\mu^\mu \propto i\overline{\psi(x)}\gamma_\mu\partial^\mu\psi(x)$ is the trace of the energy-momentum tensor. Equation (3.28) represents the vector charge conservation generalized for the deuteron states with different M [see Eqs. (2.9) and (2.10)]. In spite of a clear physical interpretation, it was recently a subject of some controversy [5–7]. Indeed, the derivation of sum rule (3.28) contains some subtle points and equivalence between it and the expression for the charge (2.8) is nontrivial particularly because of the presence of the Θ function in Eq. (3.21). This Θ function provides the correct kinematics in the variable x_N but cuts out part of the integration domain in $d^3\boldsymbol{p}$. This cutting of the integration interval in the polar angle θ leads to a nonzero contribution of the matrix element containing γ_3, which is proportional to $\cos\theta$. However, the validity of this sum rule has been firmly established [5–7]. The sum rule (3.29) for the first moment of $f_M^{N/D}$ is of a different nature; it represents the nucleon contribution to the total momentum of the deuteron [16,43,17,1] where δ_N is a part of the total momentum carried by the non-nucleon component (mesons). The constant δ_N cannot be fixed in a model-independent fashion, rather it is calculated within a particular model. Self-consistency of the theory requires that meson exchange current contribution to the deuteron SF F_2^D exactly compensates the loss of energy by nucleons in (3.29). An *important* property of sum rules (3.28) and (3.29) is that their right-hand side (RHS) does not depend on the deuteron spin orientation.

The sum rules for $f^{N/D}(y)$ and $\Delta f^{N/D}(y)$ follow from the sum rules for $f_M^{N/D}(y)$ and the definitions (3.24) and (3.25):

$$\int_0^{M_D/m} f^{N/D}(y)dy = \frac{1}{3}\sum_M \langle\gamma_0\rangle_M = \langle\gamma_0\rangle = 1, \tag{3.30}$$

$$\int_0^{M_D/m} y f^{N/D}(y)dy = \frac{1}{3}\sum_M \langle D|(\Theta_N)_\mu^\mu|D\rangle_M = 1-\delta_N, \tag{3.31}$$

$$\int_0^{M_D/m} \Delta f^{N/D}(y)dy = \langle\gamma_0\rangle_{M=1} - \langle\gamma_0\rangle_{M=0} = 0, \tag{3.32}$$

$$\int_0^{M_D/m} y\Delta f^{N/D}(y)dy = \langle D|(\Theta_N)_\mu^\mu|D\rangle_{M=1} - \langle D|(\Theta_N)_\mu^\mu|D\rangle_{M=0} = 0. \tag{3.33}$$

The sum rules for the deuteron SF's b_1^D and b_2^D are the immediate result of combining Eqs. (3.32) and (3.33) and (3.22) and (3.23):

$$\int_0^1 dx_D b_1^D(x_D) = 0, \tag{3.34}$$

$$\int_0^1 dx_D b_2^D(x_D) = 0, \tag{3.35}$$

in agreement with the sum rules suggested by Efremov and Teryaev [37].

The sum rule for the spin-dependent distribution relates the integral of the spin-dependent distribution of nucleons to the third component of the axial current (2.19) is

$$\int_0^{M_D/m} \tilde{f}^{N/D}(y)dy = \langle\gamma_5\gamma_3\rangle_{M=1}^{\mathrm{BS}}. \tag{3.36}$$

An explicit expression for the distribution function $f_M^{N/D}(y)$ [and therefore for $f^{N/D}(y)$ and $\Delta f^{N/D}(y)$] in terms of the components of the BS amplitude can be directly established from Eqs. (3.21) and (3.27) and the formulas for the corresponding densities which are given in Appendix A.

D. Calculation of distributions: Inverse Wick rotation

To calculate numerically the effective distribution functions (3.21), (3.24), (3.25), and (3.27), we need to know the matrix elements over the BS vertex functions as functions of $\boldsymbol{p}$ and $p_0 = M_D/2 - \sqrt{m^2+\boldsymbol{p}^2}$ along the real p_0 axis. The reader is reminded that the components of the BS amplitude have already been computed numerically along the imaginary axis in the p_0 plane (Wick rotation) [2,29].

In Refs. [1,3], it has been pointed out that the *moments* of the deuteron SF can be calculated in terms of the Wick rotated BS amplitude of the deuteron, since there are no extra singularities in the matrix elements describing the nucleon contribution to deep inelastic scattering other than the singularities of the amplitude itself. In principle, this implies that the SF's can be found by applying the inverse Mellin transform to the moments. In practice, however, the moments can only be calculated numerically, since the BS amplitude is known numerically. As a result, it is impossible to perform an exact inverse Mellin transform, which requires not only knowledge of an infinite number of moments but also the analytical continuation in the imaginary plane of the moments as a function of order n. These obstacles make the exact calculation of the deuteron SF impossible. Instead, one uses interpolating formulas [2,3] for the moments, which are obtained as an expansion of the exact expression for the moments in a series in p_0/m around $p_0 = 0$. This is a well-defined approximation for the moments, since in the physically interesting region, $p_0/m \ll 1$, and we can control the accuracy of the results by comparing calculations with a different number of terms. However, it is unclear how to estimate properly the accuracy of the SF, obtained by this technique of the inverse Mellin transform of interpolating formulas. We find that the deuteron SF at medium and large x, is slightly underestimated.

Now we explain the procedure for calculating the ''inverse Wick rotated'' matrix element directly for the SF, using the formalism developed in Sec. III B. We consider only the example of $f^{N/D}(y)$; other distributions are calculated in the same way. First, let us rewrite Eq. (3.21) in the form

$$f^{N/D}(y)=\frac{1}{2M_D}\int\frac{d^3\boldsymbol{p}}{(2\pi)^3}\,\delta\left(y-\frac{M_D-w+p_3}{m}\right)\Theta(y)\times[\langle\gamma_0\rangle^{\rm BS}_{\rm pole}(\boldsymbol{p}+\langle\gamma_3\rangle^{\rm BS}_{\rm pole}(\boldsymbol{p})], \tag{3.37}$$

where $\langle\gamma_0\rangle^{\rm BS}_{\rm pole}(\boldsymbol{p})$ and $\langle\gamma_3\rangle^{\rm BS}_{\rm pole}(\boldsymbol{p})$ are densities defined similarly to Eq. (2.9), but where the full integral is replaced by the contribution of the second nucleon pole, ''the nucleon pole contribution.'' Explicit forms of $\langle\gamma_0\rangle^{\rm BS}_{\rm pole}(\boldsymbol{p})$ and $\langle\gamma_3\rangle^{\rm BS}_{\rm pole}(\boldsymbol{p})$ are clear from Eqs. (3.21) and (3.37). Equation (3.37) is the *exact* form of the Eq. (3.21). Second, we notice that this density does not have any singularities in the complex plane of p_0. Nor does the matrix element

$$\begin{aligned}&{\rm Tr}\{\overline{\phi_M}(p_0,\boldsymbol{p})(\hat p_1+m)(\gamma_0+\gamma_3)(\hat p_1+m)\phi_M(p_0,\boldsymbol{p})(\hat p_2+m)\}\\&=(p_1^2-m^2)^2(p_2^2-m^2){\rm Tr}\{\overline{\Psi_M}(p_0,\boldsymbol{p})(\gamma_0+\gamma_3)\\&\quad\times\Psi_M(p_0,\boldsymbol{p})(\hat p_2-m)\}.\end{aligned} \tag{3.38}$$

Thus to calculate the nucleon pole contribution to the density, the matrix element (3.38) can be safely expanded into a Taylor series in the variable p_0 around the point $p_0=0$. Third, the coefficients of the Taylor expansion can be calculated using the known RHS of Eq. (3.38) for imaginary p_0. Finally a numerical convergence of the expansion can be checked by comparing results of calculations up to different order in p_0. Note that Eq. (3.38) and similar expressions for all other distributions are even functions of p_0; therefore, the Taylor expansion really should be done in p_0^2. In addition, the point $p_0=0$ should be a good point to expand about since, in the most physically interesting region of $|\boldsymbol{p}|/m\ll1$ we have $|p_0/m|\approx|\varepsilon_D/(2m)-|\boldsymbol{p}|^2/(2m^2)|\ll1$. The critical point for any expansion in nuclear physics is usually $|\boldsymbol{p}|/m=1$. However, even at this point $|p_0/m|$ is still a good choice for the Taylor expansion $|p_0/m|\approx|\varepsilon_D/(2m)-(\sqrt{2}-1)|\sim0.4$. For $|\boldsymbol{p}|/m\sim1.5$ the parameter $|p_0/m|$ approaches 1, and we can estimate how this limit on $|\boldsymbol{p}|$ is translated into a limit on x in the SF. To do this we perform two analytical integrations over the azimuthal and polar angles ϕ and ϑ in formula (3.37). The first integration is trivial since the integrand does not depend upon ϕ. The second integration can be done using the δ function. As a result only the integration over $|\boldsymbol{p}|$ is left, with the lower limit imposed by the integration over ϑ with the δ function

$$p_{\rm min}={\rm abs}\left(\frac{(M_D-ym)^2-m^2}{2(M_D-ym)}\right), \tag{3.39}$$

which is just a consequence of the condition $1\geqslant\cos\vartheta\geqslant-1$. Since the densities under the integral in Eq. (3.37) are very sharp functions of $|\boldsymbol{p}|$ (see, e.g., Figs. 2, 3, 6), we expect that the most important contribution to the integral comes from the region near $|\boldsymbol{p}|=p_{\rm min}$. Therefore, we estimate that the expansion in a series in p_0/m fails at the point $p_{\rm min}/m\approx1.5$,

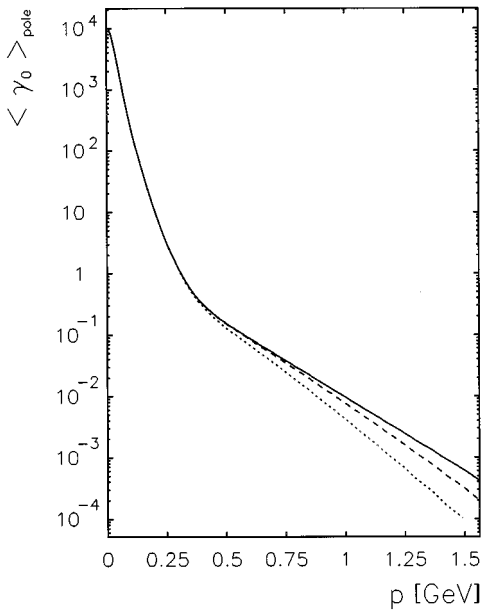

FIG. 6. The one-pole contribution to the charge density of the deuteron $\langle\gamma_0\rangle^{\rm BS}_{\rm pole}(\boldsymbol{p})$, calculated with the BS amplitude: the leading term in the Taylor expansion (dotted), first two terms up to $\propto p_0^2$ (dashed), and first three terms up to $\propto p_0^4$ (solid).

which corresponds to $y\approx1.6$ in Eq. (3.39). Finally, in accordance with the convolution formula (3.23) and taking into account that $f^{N/D}(y)$ is also a sharp function, we conclude that the method allows us to calculate the deuteron SF up to the point $x\approx1.6$. It should be remembered that this limitation is related to the restriction of the formulas by the condition $|\boldsymbol{p}|/m\sim1.5$, which is perhaps already close to the boundary of the validity domain of the *relativistic* nucleon model of the deuteron.

The results of calculations of the nucleon pole contribution to the charge density $\langle\gamma_0\rangle_{\rm pole}(\boldsymbol{p})$ are presented in Fig. 6, where we compare curves for calculations up to $\sim p_0^0$, $\sim p_0^2$, and $\sim p_0^4$. As we expected, the procedure is nicely convergent up to $|\boldsymbol{p}|\sim1$ GeV and with reasonable accuracy can be used up to $|\boldsymbol{p}|\sim1.5$ GeV. Similar results for the pole contribution to the axial density $\langle\gamma_5\gamma_3\rangle_{\rm pole}(\boldsymbol{p})$ are shown in Fig. 7.

Note that the numerical approximations made in this section, such as limiting number of terms in the Taylor expansion, can potentially lead to a numerical violation of the exact sum rules.

E. Nonrelativistic formulas for structure functions

The nonrelativistic expressions for $f^{N/D}(y)$, $\Delta f^{N/D}(y)$, and $\vec f^{N/D}(y)$ can be obtained by using an analogy of the charge densities calculated within the BS formalism and the corresponding densities calculated with wave functions [e.g., Eqs. (2.11), (2.13), (2.15), and (2.16)]. Actually, the distributions in the BS formalism are expressed in terms of nucleon pole contributions to the densities in the nucleon pole approximation (3.21), (3.25), and (3.27), and not the exact densities as in Eq. (2.9). However, in order to obtain the nonrelativistic approximation to the relativistic formulas, one can use the fact that the nucleon pole contribution gives the main contribution to the density, at least in the nonrela-

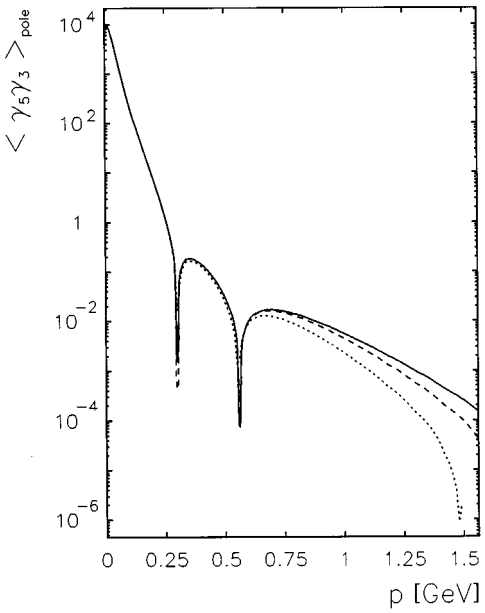

FIG. 7. The one-pole contribution to the spin density, of the deuteron $\langle \gamma_5\gamma_3 \rangle^{\rm BS}_{\rm pole}(\boldsymbol{p})$ calculated with the BS amplitude: the leading term in the Taylor expansion (dotted), first two term, up to $\propto p_0^2$ (dashed), and first three term, up to $\propto p_0^4$ (solid).

tivistic region. Such an assumption is very common in nuclear physics (see, e.g., [20,22,44,10,11]). For instance, the well-known result for the spin-independent distribution is immediately reproduced (see, e.g., [17,8,16]):

$$f^{N/D}_{\rm NR}(y) = \int \frac{d^3\boldsymbol{p}}{(2\pi)^3}\,\delta\!\left(y-\frac{M_D-w+p_3}{m}\right) \times\Theta(y)\{\langle\gamma_0\rangle^{\rm NR}(\boldsymbol{p})+\langle\gamma_3\rangle^{\rm NR}(\boldsymbol{p})\} = \int \frac{d^3\boldsymbol{p}}{(2\pi)^3}\,\delta\!\left(y-\frac{M_D-w+p_3}{m}\right) \times\Theta(y)\left(1+\frac{|\boldsymbol{p}|\cos\theta}{m}\right)\{u^2(|\boldsymbol{p}|)+w^2(|\boldsymbol{p}|)\}. \tag{3.40}$$

The presence of the Θ function on the RHS of Eq. (3.40) slightly violates the sum rule (3.30). However, this is not noticeable phenomenologically, since only the region of large momenta $|\boldsymbol{p}|>0.7$ GeV is affected by the Θ function and it does not contribute much to the norm of the deuteron wave function. We can accept this slight effect of the Θ functions, since a nonrelativistic approximation is based on the belief that high momenta are not important.

For distribution $\Delta f^{N/D}(y)$, we get

$$\Delta f^{N/D}_{\rm NR}(y) = -\int \frac{d^3\boldsymbol{p}}{(2\pi)^3}\,\delta\!\left(y-\frac{M_D-w+p_3}{m}\right)\Theta(y) \times\left(1+\frac{|\boldsymbol{p}|\cos\theta}{m}\right)P_2(\cos\theta)\frac{3}{2}w(|\boldsymbol{p}|) \times\{2\sqrt{2}u(|\boldsymbol{p}|)+w(|\boldsymbol{p}|)\}. \tag{3.41}$$

Again, the sum rule (3.32) is broken by the presence of the Θ function in Eq. (3.41). Neglecting it, one obtains

$$\int_0^1 dx_D b_1^D(x_D) \propto \int_0^{M_D/m} \Delta f^{N/D}_{\rm NR}(y)dy \propto \int_{-1}^1 d(\cos\theta)\left(1+\frac{|\boldsymbol{p}|\cos\theta}{m}\right)P_2(\cos\theta)=0, \tag{3.42}$$

where the orthogonality property of the Legendre polynomials is used.

A deviation from zero caused by the Θ functions is not large compared to 1. One can *artificially* adjust formula (3.41) to satisfy this sum rule. For instance, *small* corrections to the normalization of both terms with $M=1$ and $M=0$ can be made to satisfy the sum rule in the form (3.32). However, the situation with the second sum rule (3.35) is more difficult and cannot be fixed by any simple adjustments of the normalizations or by ignoring the Θ functions. As for Eq. (3.42), one can write (neglecting the Θ function)

$$\int_0^1 dx_D b_2^D(x_D) \propto \int_0^{M_D/m} y\Delta f^{N/D}_{\rm NR}(y)dy \propto \int_{-1}^1 d(\cos\theta)(M_D-w+|\boldsymbol{p}|\cos\theta) \times\left(1+\frac{|\boldsymbol{p}|\cos\theta}{m}\right)P_2(\cos\theta)\neq 0. \tag{3.43}$$

There is no reason for this sum rule to be satisfied with the nonrelativistic distribution function (3.41). Therefore the nonrelativistic formulas, in principle, violate the sum rules for the SF's $b^D_{1,2}$.

The nonrelativistic formulas for the other spin-dependent distribution $\vec{f}^{N/D}$ are also a straightforward result of using densities (2.16) instead of the relativistic densities in Eq. (3.27) [see also footnote to the formula (2.19)]:

$$\vec{f}^{N/D}_{\rm NR}(y) = \int \frac{d^3\boldsymbol{p}}{(2\pi)^3}\,\delta\!\left(y-\frac{M_D-w+p_3}{m}\right) \times\Theta(y)\left\{u^2(|\boldsymbol{p}|)-\frac{1}{2}w^2(|\boldsymbol{p}|) +P_2(\cos\vartheta)w(|\boldsymbol{p}|)[w(|\boldsymbol{p}|)-\sqrt{2}u(|\boldsymbol{p}|)]\right\}. \tag{3.44}$$

The sum rule that follows from Eq. (2.18) is

$$\int_0^{M_D/m} \vec{f}^{N/D}_{\rm NR}(y)dy = 1-\frac{3}{2}w_D. \tag{3.45}$$

F. Calculation of distributions: Relativistic vs nonrelativistic

In order to understand if the relativistic distribution functions (3.21), (3.25), and (3.27) are significantly different from the nonrelativistic distributions (3.40), (3.41), and

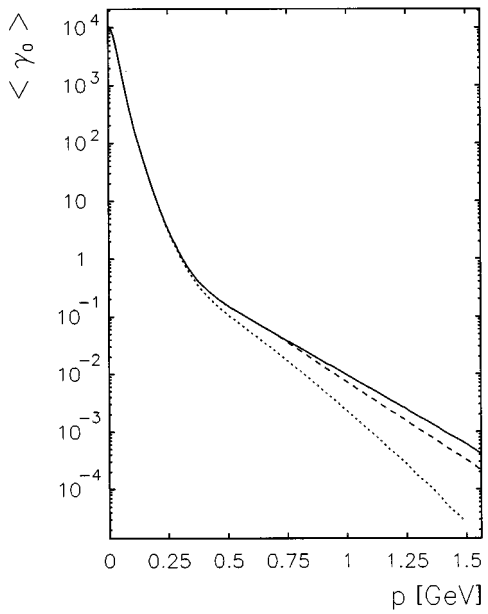

FIG. 8. Different ''versions'' of the charge density of the deuteron calculated with the BS amplitude: exact $\langle \gamma_0 \rangle^{\rm BS}(\boldsymbol{p})$ (dotted), in the pole approximation $\langle \gamma_0 \rangle^{\rm BS}_{\rm pole}(\boldsymbol{p})$ (solid). The dashed curve presents the effective density for deep inelastic scattering which is the density in the pole approximation including the Θ function cutoff at high momenta.

(3.27), we have to understand fully the effect of the one pole approximation on the densities in the BS formalism. Indeed, the discussion of Sec. II B suggested that we cannot expect significant physical effects from the form of the densities, since both relativistic and nonrelativistic *realistic* models lead to similar results and we do not find any special behavior in the relativistic model.

In Figs. 8 and 9 we compare the full densities and the nucleon pole contributions to the densities, for the two most

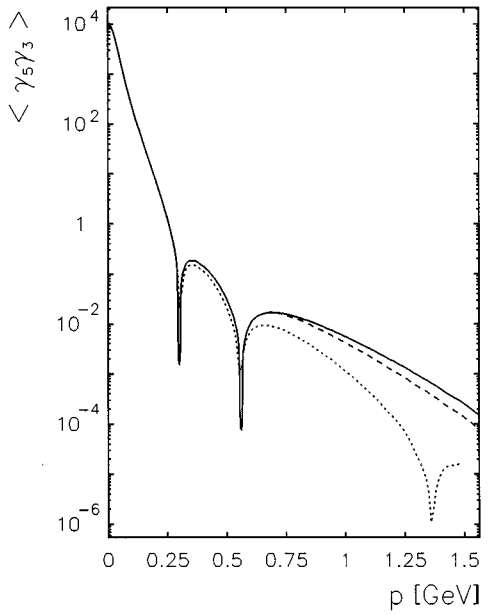

FIG. 9. The same as in Fig. 8, but for the spin-density $\langle \gamma_5 \gamma_3 \rangle^{\rm BS}(\boldsymbol{p})$.

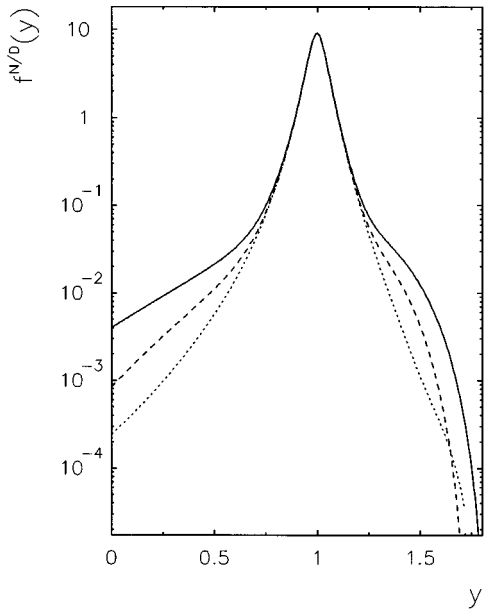

FIG. 10. The effective distribution for the nucleon contribution in the deuteron structure function F_2^D, $f^{N/D}(y)$: fully relativistic BS (solid), nonrelativistic Bonn (dotted), and nonrelativistic calculation using the BS charge density (dashed).

important cases $\langle \gamma_0 \rangle$ and $\langle \gamma_5 \gamma_3 \rangle$ and find that the one pole approximation leads to a significant change in the density. The nucleon pole contribution to the densities (solid curves) have a much harder tail compared to the exact densities (dotted curves), starting at $|\boldsymbol{p}| \sim 0.5m$, and this leads to an order of magnitude larger effect at $|\boldsymbol{p}| \sim 1.5m$. This can be qualitatively understood by considering an example of the charge density $\langle \gamma_0 \rangle$. Indeed, selecting only the nucleon pole contribution in the full integral corresponds to neglecting the antinucleon (negative) contribution to the total charge density which is concentrated at high momenta $|\boldsymbol{p}|$. The presence of Θ functions in the expressions for the distribution function $f^{N/D}$ and $\tilde{f}^{N/D}$ cuts off a part of the high momentum region, but this is a minor effect. The ''softening'' caused by the Θ functions is also illustrated in Figs. 8 and 9 (dashed lines). These curves are the BS densities obtained in the pole approximation (solid lines) multiplied by $\Theta(M_D - \omega + p_3)$ and integrated over $\cos\theta$.

The results presented in Figs. 8 and 9 imply that the relativistic densities appearing in the formulas for the effective distribution functions are enhanced at medium and high momenta. Comparing these results with those in Figs. 2 and 5 we find that the effect is much larger than any model differences. Still, since the effect is concentrated at high momenta, it is not clear if it leads to observable effects in deep inelastic scattering. To clarify this, in Fig. 10 we present the effective distribution function $f^{N/D}(y)$. For completeness we compare distribution functions calculated using three different charge densities: (i) the nonrelativistic density of the Bonn potential (dotted line), (ii) the nucleon pole contribution to the relativistic BS density (solid curve), and (iii) the full density within the BS approach (dashed curve). The last curve is intended to illustrate differences in the description of the *mechanism* of the reaction in nonrelativistic and relativistic approaches. In this case the charge density of the nonrelativistic model is

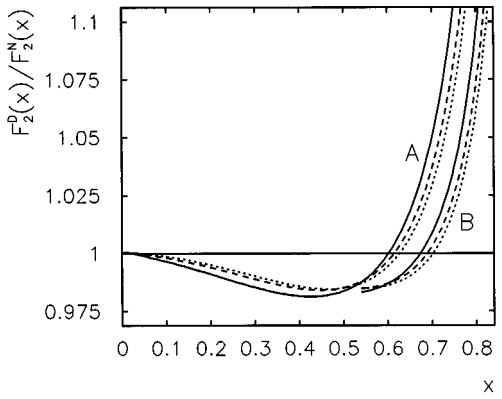

FIG. 11. The ratio of the deuteron and nucleon structure functions F_2^D/F_2^N calculated in different models. The curves correspond to the three effective distributions from Fig. 10: fully relativistic BS (solid), nonrelativistic Bonn (dotted), and nonrelativistic calculation using the BS charge density (dashed). The two groups of curves correspond to different parametrizations of the nucleon SF $F_2^N \sim (1-x)^\gamma$: $\gamma \approx 3.2$ from Ref. [45] A; $\gamma = 2.7$, see Refs. [2,17] B.

assumed exactly the same as that of the BS approach. We find that a consistent relativistic description gives an effective distribution which is systematically harder at high values of the momentum fraction y. This is a result of the harder tail contribution of the nucleon pole term. It is interesting to note that the relativistic distribution is also enhanced at $y \to 0$. This effectively corresponds to the larger ''binding effects'' in the BS approach which was observed in Ref. [2]. Very similar effects can be observed in the other effective distribution functions $\tilde{f}^{N/D}$ and $\Delta f^{N/D}$. However, in these cases the effects are not as evident because of the oscillating nature of the distribution functions. (See, e.g., discussion about $\Delta f^{N/D}$ below.)

IV. NUMERICAL CALCULATION OF STRUCTURE FUNCTIONS

A. Unpolarized deuteron F_2^D

The spin-independent SF of the deuteron F_2^D is calculated using the effective distribution functions presented in Fig. 10 (see discussion at the end of the Sec. III F). The results are shown in Fig. 11 in the form of ratio of the corresponding SF of the deuteron and the nucleon. The nucleon SF F_2^N is taken from Ref. [45] at $Q^2 = 10\ \mathrm{GeV}^2$ (the group of curves A). We find that the BS approach gives a behavior of the deuteron SF qualitatively similar to the results of the nonrelativistic calculations and those in which the nonrelativistic charge density is used in this BS approximation. However, there are two delicate, but essential differences.

First, the ratio F_2^D/F_2^N in the BS approach is less than in the other calculations at small x, $x < 0.5$. This effect can be easily understood from the form of the distribution $f^{N/D}(y)$ in Fig. 10 and formula (3.23). Indeed, at $x = 0$ the SF F_2^D is

$$F_2^D(0) = F_2^N(0) \int_0^{M_D/m} f^{N/D}(y)\,dy. \tag{4.1}$$

Therefore $F_2^D(0)/F_2^N(0) = 1$ since

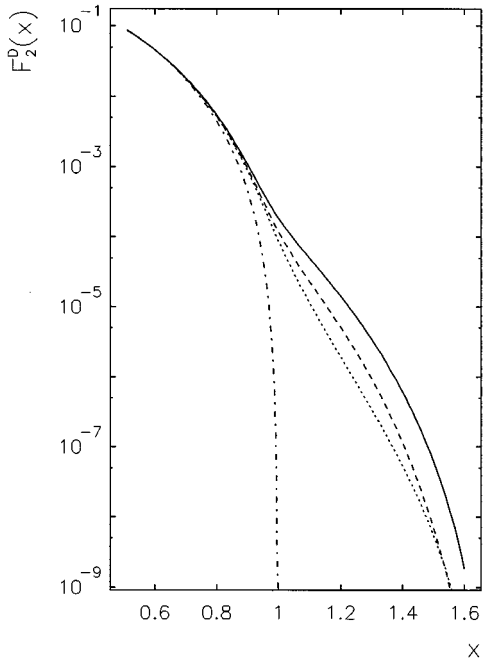

FIG. 12. The deuteron structure function $F_2^D(x)$ at large x calculated in different models. Curves correspond to three effective distributions from Fig. 10: fully relativistic BS (solid), nonrelativistic Bonn (dotted), and nonrelativistic calculation using the BS charge density (dashed). Dash-dotted curve presents the free nucleon structure function F_2^N.

$$\int_0^{M_D/m} f^{N/D}(y)\,dy = 1$$

is a normalization from Eq. (3.30). When we move from $x = 0$ to larger x, we ''lose'' part of the normalization, since the lower limit of the integral in Eq. (3.23) is x. Since the relativistic $f^{N/D}$ is larger at small x than in the nonrelativistic case, it leads to a faster decrease of the relativistic SF with increasing x. The fact that the ratio F_2^D/F_2^N is less than 1 at small and intermediate x is known to be a result of the ''binding of nucleons'' (see, e.g., [15–17,1] and references therein).

Second, the relativistic SF displays a sharper rise at higher x, $x > 0.5$ than in the nonrelativistic case. Again, this can be understood from the form of the distribution as seen in Fig. 10, and the convolution formula (3.23). With increasing x the role of the high momentum tail of the effective distribution gains more importance in the integration in Eq. (3.23) and at $x > 1.0$ the tail is completely dominant. The deuteron SF at $x > 1$ is presented in Fig. 12.

It has been shown recently that relativistic calculations lead to larger binding effects than in nonrelativistic calculations [13,2]. However, the result of Ref. [13], which indicates effects two to three times larger than ours is still neither explained nor physically understood. In Ref. [2] the size of the effect was not so very large, but the method of numerical calculations was essentially based on the *numerical* inverse Mellin transform of a nonanalytical function. Approximations with limited validity at high momentum were made. This led to special efforts to verify the quantitative size of the effect. It is worthwhile to remember that we have already

pointed out a tiny effect of $\sim 1-2\,\%$ in the ratio F_2^D/F_2^N. We can also measure the binding effect using the energy-momentum sum rule (3.29). The quantity δ_N is a natural parameter controlling the binding in any calculation. For example, the nonrelativistic formulas allow for an analytical estimate of δ_N which essentially gives us the size of this effect [16,17,2]

$$\delta_N = \frac{\varepsilon_D}{m} - \frac{\langle T\rangle}{6m}. \tag{4.2}$$

Here $\langle T\rangle$ is the nonrelativistic mean kinetic energy of nucleons in the deuteron. For the realistic models typically $\langle T\rangle \approx 15$ MeV, which gives $\delta_N \approx 5\times 10^{-3}$. Calculating with the BS effective distribution of the present paper we find $\delta_N \approx 0.7\times 10^{-3}$. Note that in Ref. [2] the quantity $\delta_N \approx 1\times 10^{-2}$ has been reported. We attribute this small discrepancy to the poorer numerical approximation which were made in [2]. This approximation underestimates a high momentum behavior of $f^{N/D}$, however, phenomenologically the effect is not significant (cf. Ref. [2]).

To illustrate the dependence of ratio F_2^D/F_2^N on the parametrization of the ''elementary'' nucleon SF, we also present the results of the calculation at $x>0.5$, utilizing the different parametrization of F_2^N (see Refs. [2,17]) shown in Fig. 11 (the group of curves B). A noticeable difference from earlier calculations (group of curves A) is the shift of the point $F_2^D(x)/F_2^N(x)=1$ from $x^*\approx 0.6$ to $x^*\approx 0.7$. This difference is caused by the difference in the asymptotic behavior of the two parametrizations in the form

$$F_2^N(x) \sim C(1-x)^{\gamma}, \tag{4.3}$$

with $\gamma \approx 3.2$ for case A and $\gamma \approx 2.7$ for case B. To understand this ''instability,'' we evaluate $F_2^D(x)$, Eq. (3.23), by expanding $F_2^N(x/y)$, Eq. (4.3), in a Taylor series around $\langle y\rangle$, the point of the sharp maximum of the effective distribution $f^{N/D}(y)$

$$\langle y\rangle = \int_0^{M_D/m} y f^{N/D}(y)\,dy. \tag{4.4}$$

It is sufficient to keep terms up to the second derivatives of F_2^N, and the result in this case contains only the first and second moments of $f^{N/D}(y)$. The nonrelativistic estimate for the moments of $f^{N/D}(y)$ [1,17] gives

$$\begin{aligned}\langle y^n\rangle &\equiv \int_0^{M_D/m} y^n f^{N/D}(y)\,dy \\ &\simeq 1+\frac{1}{6}n^2\frac{\langle T\rangle}{m}+\frac{2}{3}n\frac{\langle T\rangle}{m}+n\frac{\langle V\rangle}{m},\end{aligned} \tag{4.5}$$

where $\langle T\rangle$ is the mean kinetic energy of nucleons in the deuteron, and $\langle V\rangle = \varepsilon_D - \langle T\rangle$ is the mean potential in the deuteron. Finally, the crossover point x^* is defined as

$$x^* = \frac{3(\langle T\rangle + 2\langle V\rangle)}{(4-\gamma)\langle T\rangle + 6\langle V\rangle}. \tag{4.6}$$

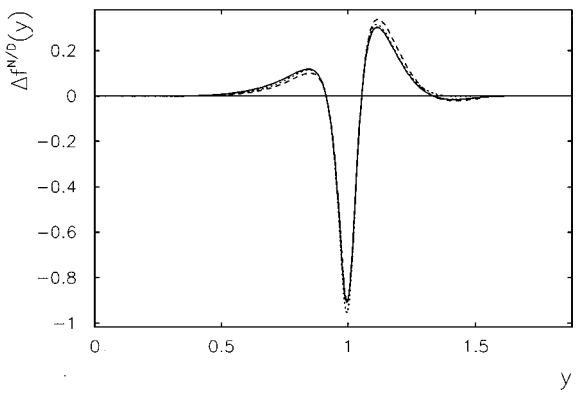

FIG. 13. The effective distribution functions for the deuteron structure functions $b_{1,2}^D$ and $\Delta f^{N/D}(y)$ calculated in different models: fully relativistic BS (solid) and nonrelativistic Bonn (dotted). The dashed curve presents $y\Delta f^{N/D}(y)$.

Using typical values of $\langle T\rangle \approx 15$ MeV and $\varepsilon_D \approx -2.2$ MeV, we find that varying γ from 2.7 to 3.2 leads to changing x^* from ≈ 0.7 to ≈ 0.63. Therefore this estimate is in reasonable agreement with the exact results in Fig. 11. Thus, we find that the position of the crossover point x^* depends both on nuclear effects, through $\langle T\rangle$ and $\langle V\rangle$, and on the form of the nucleon SF, through γ. Therefore, the exact position of x^* is not a feature attributed to a particular model of the deuteron. Still, an explicit interplay of the nuclear and nucleon effects in Eq. (4.6) shows that a *consistent* analysis is required in order to extract accurate information about the nucleon SF from the deuteron data [45].

B. Polarized deuteron b_1^D and b_2^D

The SF's of the deuteron $b_{1,2}^D(x)$ are calculated within both the relativistic and nonrelativistic approaches. The relativistic calculations are based on formulas (3.21), (3.22)–(3.25). The nonrelativistic calculations, Eq. (3.41), use the realistic wave function of the deuteron obtained from the Bonn potential [19]. The nucleon SF's $F_{1,2}^N(x,Q^2)$, is again taken from Ref. [45] at $Q^2=10$ GeV^2. The results are neither very sensitive to the particular choice of the parametrization of the nucleon SF's nor to their Q^2 dependence.

The distribution functions $\Delta f^{N/D}(y)$ are calculated and the results are presented in Fig. 13. Similar behavior of the distribution function is obtained in both the relativistic (solid line) and nonrelativistic (dotted line) calculations. Indeed, it is difficult to distinguish between them, let alone make any definite conclusions. The third line in the Fig. 13 is given for illustration as it presents $y\Delta f^{N/D}(y)$ for the relativistic calculations. The calculation of the sum rules is more representative. To understand the scale of effects, which are discussed below, it is customary to define the auxiliary quantity

$$\begin{aligned}\int_0^{M_D/m} \mathrm{abs}[\Delta f^{N/D}(y)]\,dy &\simeq \int_0^{M_D/m} \mathrm{abs}[y\Delta f^{N/D}(y)]\,dy \\ &\simeq 0.14.\end{aligned} \tag{4.7}$$

The BS and nonrelativistic Bonn calculations give the same result in Eq. (4.7), within $\sim 5\%$. Thus, the effective distribution functions $\Delta f^{N/D}$ are an order of magnitude smaller

than the usual spin-independent distributions $f^{N/D}$ which is normalized to 1. This is not very important, but it decreases the accuracy in the numerical calculations, since $\Delta f^{N/D}$ is a difference of two functions each normalized to 1 ($M=1$ and $M=0$). Numerically the sum rule (3.34) [see also Eq. (3.42)] is satisfied both in relativistic and nonrelativistic calculations with good accuracy despite the approximate numerical ''inverse Wick rotation.'' The corresponding integrals are $\sim 5\times 10^{-4}$ and $\sim 3\times 10^{-5}$ and they should be compared to the estimate (4.7). The sum rule (3.28) may be used to improve distributions $\Delta f^{N/D}$ by making integrals for $f_1^{N/D}$ and $f_0^{N/D}$ *exactly* the same. However, this does not lead to a significant variation of results for SF's except for $x\to 0$ for $b_1^D(x)$.

The behavior of $b_1^D(x)$ at $x\to 0$ deserves to be considered more closely, especially for numerical calculations, since the nucleon function $F_1^N(x)$ can be divergent at small x. Unfortunately it is impossible to calculate $b_1^D(0)$ exactly for the realistic SF F_1^N. However, a contribution of the singularity can be evaluated. Indeed, let us assume a singular behavior of $F_1^N\sim C/x$, then for small x, Eq. (3.22) leads to

$$b_1^D(x\to 0)\sim \frac{C}{x}\int_x^{M_D/m}\Delta f^{N/D}(y)dy$$
$$=\frac{C}{x}\left\{\int_0^{M_D/m}-\int_0^x\right\}\Delta f^{N/D}(y)dy$$
$$\sim\frac{CZ}{x}-C\Delta f^{N/D}(0), \tag{4.8}$$

where $Z=0$ in the exact relativistic formula. It can still be a small number in numerical calculations or in the nonrelativistic case. Thus, the limit of the deuteron SF $b_1^D(x)$ as $x\to 0$ is a constant, but one has to exercise great care in performing numerical computations since any error leads to a divergent behavior at small x. In this context, an adjustment of the norms of the two terms in formulas (3.25) and (3.41) means the subtraction of the numerical error from b_1^D at small x.

The situation with the second sum rule (3.35) is quite different. Numerically it is violated more significantly than in the previous case. The corresponding integrals are $\sim 1\times 10^{-3}$ and $\sim 3\times 10^{-3}$ for relativistic and nonrelativistic calculations, respectively, i.e., about 0.7 and 2 % compared to Eq. (4.7). Therefore, numerical approximations adversely affect the relativistic formula also. This is attributed to the numerical rotation in the Minkowski space. An adjustment of the normalization, as it has been discussed, slightly improves the accuracy (to 0.5%). On the other hand, the result for the nonrelativistic approach is stable with respect to any adjustments since it is defined by the formulas (3.43).

The SF's b_1^D and b_2^D are calculated within the two approaches. The results are shown in Figs. 14(a) and 14(b). The behavior of the functions in Fig. 14(a) suggests the validity of the sum rule (3.34). At the same time, the nonrelativistic calculation for b_2^D in Fig. 14(b) (dotted line) obviously does not satisfy the sum rule (3.35). The main difference of the relativistic and nonrelativistic calculations is at small x, where these approaches give different signs for the SF's. To illustrate the effect of the presence of the Θ function under the integral in the nonrelativistic formula (3.41), the calculations have also been performed with a restricted interval of integration over $|\boldsymbol{p}|$. The condition $|\boldsymbol{p}|<0.7$ GeV corresponds to a ''softer'' deuteron wave function, but makes the sum rule (3.43) exact. Corresponding SF's are shown in Figs. 14(a) and 14(b) (dashed line). The result of this ''experiment'' is that the effect of the Θ function is not quantitatively significant. It also does not affect the principle conclusion about the second sum rule (3.35), but makes the defect a little smaller. This is understandable since the sum rule breaking term in Eq. (3.43) is $\propto|\boldsymbol{p}|\cos\theta$.

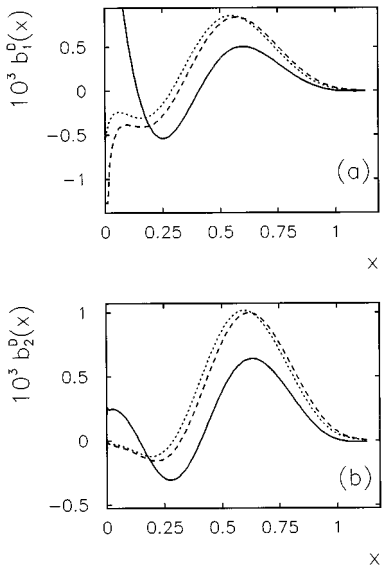

FIG. 14. The deuteron structure functions b_1^D (a) and b_2^D (b) calculated in different models: fully relativistic BS (solid), and nonrelativistic Bonn (dashed). The dotted curve presents $b_{1,2}^D$ calculated with the ''soft'' nucleon distribution, the Bonn distribution, but cutoff at $|\boldsymbol{p}|>0.7$ GeV .

C. Polarized deuteron g_1^D

The spin-dependent SF of the deuteron g_1^D is calculated using the same three models as the spin-independent SF F_2: the fully relativistic BS approach (solid line), the nonrelativistic approach based on the Bonn wave function (dotted line), and the nonrelativistic approach which uses the exact density of the BS approach (dashed line). The nucleon SF g_1^N is taken from Ref. [46]. The results of calculations are presented in Fig. 15.

For illustration we also present in Fig. 15 the quantity $\langle\gamma_5\gamma_3\rangle_{M=1}^{\rm BS}$ which corresponds to a ''model'' for the deuteron SF (dot-dashed straight line):

$$g_1^D(x,Q^2)=\frac{1}{4\pi}\langle\gamma_5\gamma_3\rangle_{M=1}^{\rm BS}g_1^N(x,Q^2). \tag{4.9}$$

If we replace $\langle\gamma_5\gamma_3\rangle_{M=1}^{\rm BS}$ by the factor $(1-3/2w_D)$ from Eq. (2.18) we get the formula usually used by experimentalists to obtain the neutron SF g_1^n from the combined proton and deuteron data.

Figure 15 shows that this is different from the naive estimate (4.9). However, within the present day experimental errors it may be *a reasonable approximation* (see, e.g., Ref. [4]). Huge jumps of the ratio around the constant $\langle\gamma_5\gamma_3\rangle_{M=1}^{\rm BS}$

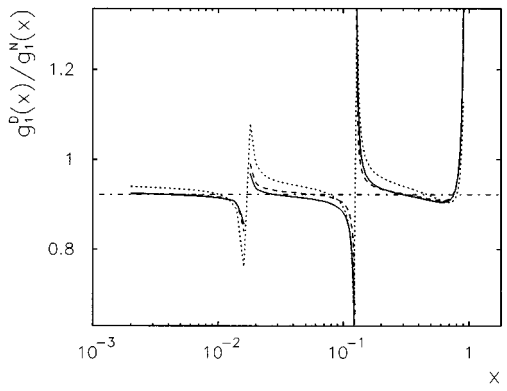

FIG. 15. The ratio of the deuteron and nucleon spin-dependent structure functions g_1^D/g_1^N calculated in different models. Curves correspond to three effective distributions: fully relativistic BS (solid), nonrelativistic Bonn (dotted), and nonrelativistic, but using the BS spin density (dashed).

at $x<0.7$ are not too important. They correspond to zeros of the nucleon SF which are slightly shifted by the convolution formula. A systematic difference in the ratio exists between the nonrelativistic calculation (dotted line) and the two calculations based on the BS densities (solid and dashed curves). This arises from the difference between the D-wave admixture in the Bonn potential ($w_D \approx 4.3\%$) and in our solution of the BS equation ($w_D \approx 5\%$). The rise of the ratio, at x greater than 0.7, is of the same nature as in the spin-independent case in Fig. 11; it is caused by the Fermi motion.

V. SUMMARY

In this paper, we have presented a study of the deep inelastic electron scattering on the deuteron in the Bethe-Salpeter formalism in the realistic meson-nucleon model. In particular:

(1) The connection of the structure functions to the densities of the appropriate charges and currents is analyzed. By analyzing the same densities in the nonrelativistic approach, we have systematically compared the relativistic and nonrelativistic calculations, and established sources of the relativistic effects.

(2) Using our numerical solution of the Bethe-Salpeter equation amplitude with a realistic kernel, the leading-twist structure functions of the deuteron F_2^D, $b_{1,2}^D$, and g_1^D, are calculated in a fully relativistic fashion.

(3) Our numerical calculations of the structure functions emphasize a qualitative agreement with previous nonrelativistic results. However, we have found effects that systematically distinguish a consistent relativistic approach from the nonrelativistic one: in the relativistic formalism (i) the magnitude of binding effects is larger, (ii) the effect of Fermi motion at high x is stronger, and (iii) the nonrelativistic calculations suffer unavoidable internal inconsistencies which lead to small effects in the structure functions F_2^D and g_1^D, but seriously affect the structure function $b_{1,2}^D$ and noticeably violate sum rules for this function.

The present paper concludes our systematic study of the deep inelastic electron (muon) scattering on the deuteron in the Bethe-Salpeter formalism. The results are collected in the two papers, Ref. [1] and the present paper, and in part have also been published previously in Refs. [2–4,30]. The main lesson we have learned from this study is that the deuteron in the deep inelastic reaction indeed behaves as a very slightly relativistic system. One has to look for special conditions or kinematics of the reaction to be able to find noticeable relativistic effects. We have found certain situations where the relativistic approach is absolutely essential and use of the nonrelativistic methods is not justified. Most representative examples are the high x behavior of the structure functions and the spin-dependent structure functions $b_{1,2}^D$.

Apart from the phenomenological differences between the relativistic and nonrelativistic approaches, the most important merit of the covariant formalism is its *consistency*. Its close connection to field theory guarantees that the calculated observables obey the sum rules and other general properties imposed by fundamental principles. In this sense the relativistic approach is definitely more advanced theoretically than its nonrelativistic counterpart and provides a better understanding of deep inelastic scattering on the deuteron.

ACKNOWLEDGMENTS

We would like to thank F. Gross, W. Van Orden, and J. Tjon for conversations about properties of the relativistic equations and their solutions. The authors also wish to thank everybody who discussed various topics of this paper with us. In particular, we would like to thank S. Bondarenko, V. Burov, C. Ciofi degli Atti, S. Dorkin, A. Efremov, B. Kämpfer, K. Kazakov, S. Kulagin, W. Melnitchouk, A. Molochkov, S. Scopetta, C. Shakin, S. Simula, O. Teryaev, A. Titov, A. Thomas, and W. Weise. We wish to express our sincere thanks to Professor G. Greeniaus, Professor H. G. Miller, and Dr. A. Mcpherson for a careful reading of the manuscript. The research was supported in part by the Natural Sciences and Engineering Research Council of Canada and by Instituto Nazionale di Fisica Nucleare, Sezione di Perugia, Italy.

APPENDIX A: EXPLICIT FORMULAS FOR DENSITIES

In this appendix we present formulas which allow us to restore the explicit form of the various densities in the BS formalism. For convenience, we define the auxiliary ''densities''

$$\begin{Bmatrix} f_0^{N/D}(p) \\ f_3^{N/D}(p) \end{Bmatrix} = \frac{1}{3}\sum_M \int_0^{2\pi} d\phi \mathrm{Tr}\left\{ \overline{\Psi}_M(p_0,\boldsymbol{p}) \begin{Bmatrix} \gamma_0 \\ \gamma_3 \end{Bmatrix} \Psi_M(p_0,\boldsymbol{p})(\hat{p}_2 - m) \right\}, \tag{A1}$$

$$\begin{Bmatrix} \Delta f_0^{N/D}(p) \\ \Delta f_3^{N/D}(p) \end{Bmatrix} = \int_0^{2\pi} d\phi \mathrm{Tr}\left\{ \overline{\Psi}_M(p_0,\boldsymbol{p}) \begin{Bmatrix} \gamma_0 \\ \gamma_3 \end{Bmatrix} \Psi_M(p_0,\boldsymbol{p})(\hat{p}_2 - m) \right\}_{M=1} - \int_0^{2\pi} d\phi \mathrm{Tr}\{\cdots\}_{M=0}, \tag{A2}$$

$$\begin{Bmatrix} \vec{f}_0^{N/D}(p) \\ \vec{f}_3^{N/D}(p) \end{Bmatrix} = \int_0^{2\pi} d\phi \mathrm{Tr}\left\{ \overline{\Psi_M}(p_0,\boldsymbol{p}) \begin{Bmatrix} \gamma_5\gamma_0 \\ \gamma_5\gamma_3 \end{Bmatrix} \Psi_M(p_0,\boldsymbol{p})(\hat{p}_2 - m) \right\}_{M=1}, \tag{A3}$$

where integration over ϕ leads to the trivial factor of 2π since none of the matrix elements on the RHS depends on ϕ. To obtain explicit expressions for the densities discussed in the paper we have to compare Eqs. (A1)–(A3) with definitions of the corresponding densities.

Note that the formalism presented in Refs. [1,2] and in this paper can be easily adopted to analytical computer calculations. The following results have been obtained utilizing the MATHEMATICA package [47]:

$$\begin{aligned} f_0^{N/D}(p) = m[&-8\psi_{a0}(p_0,p)\psi_{t0}(p_0,p) - 8\psi_{a2}(p_0,p)\psi_{t2}(p_0,p)] + p\left(\frac{-8\psi_{p1}(p_0,p)\psi_{t0}(p_0,p)}{\sqrt{3}} + 8\sqrt{\frac{2}{3}}\psi_{p1}(p_0,p)\psi_{t2}(p_0,p) \right. \\ &\left. + 4\sqrt{\frac{2}{3}}\psi_{a0}(p_0,p)\psi_{v1}(p_0,p) + \frac{4\psi_{a2}(p_0,p)\psi_{v1}(p_0,p)}{\sqrt{3}} \right) + \left(\frac{1}{2}M_d - p_0 \right)[2\psi_{a1}^0(p_0,p)^2 + 2\psi_{a0}(p_0,p)^2 \\ &+ 2\psi_{a2}(p_0,p)^2 + 2\psi_{p1}(p_0,p)^2 + 8\psi_{t0}(p_0,p)^2 + 8\psi_{t2}(p_0,p)^2 + 8\psi_{t1}^0(p_0,p)^2 + 2\psi_{v1}(p_0,p)^2], \end{aligned} \tag{A4}$$

$$\begin{aligned} f_3^{N/D}(p) = \cos(\theta)\Bigg\{ &\left(\frac{1}{2}M_d - p_0 \right)\left(\frac{8\psi_{p1}(p_0,p)\psi_{t0}(p_0,p)}{\sqrt{3}} - 8\sqrt{\frac{2}{3}}\psi_{p1}(p_0,p)\psi_{t2}(p_0,p) - 4\sqrt{\frac{2}{3}}\psi_{a0}(p_0,p)\psi_{v1}(p_0,p) \right. \\ &\left. - \frac{4\psi_{a2}(p_0,p)\psi_{v1}(p_0,p)}{\sqrt{3}} \right) + m\left(\frac{-4\psi_{a0}(p_0,p)\psi_{p1}(p_0,p)}{\sqrt{3}} + 4\sqrt{\frac{2}{3}}\psi_{a2}(p_0,p)\psi_{p1}(p_0,p) \right. \\ &\left. + 8\sqrt{\frac{2}{3}}\psi_{t0}(p_0,p)\psi_{v1}(p_0,p) + \frac{8\psi_{t2}(p_0,p)\psi_{v1}(p_0,p)}{\sqrt{3}} \right) + p\left(2\psi_{a1}^0(p_0,p)^2 - \frac{2\psi_{a0}(p_0,p)^2}{3} \right. \\ &- \frac{8\sqrt{2}\psi_{a0}(p_0,p)\psi_{a2}(p_0,p)}{3} + \frac{2\psi_{a2}(p_0,p)^2}{3} - 2\psi_{p1}(p_0,p)^2 + \frac{8\psi_{t0}(p_0,p)^2}{3} - 2\psi_{v1}(p_0,p)^2 \\ &\left. + \frac{32\sqrt{2}\psi_{t0}(p_0,p)\psi_{t2}(p_0,p)}{3} - \frac{8\psi_{t2}(p_0,p)^2}{3} + 8\psi_{t1}^0(p_0,p)^2 \right) \Bigg\}, \end{aligned} \tag{A5}$$

$$\begin{aligned} \vec{f}_0^{N/D}(p) = \Bigg\{ &\frac{M_d}{2}\left(\frac{1}{2}M_d - {p_0}^2 \right)[\sqrt{6}\psi_{a0}(p_0,p)\psi_{v1}(p_0,p) + 2\sqrt{3}\psi_{a2}(p_0,p)\psi_{v1}(p_0,p)] + m[-4\sqrt{6}\psi_{t0}(p_0,p)\psi_{v1}(p_0,p) \\ &- 4\sqrt{3}\psi_{t2}(p_0,p)\psi_{v1}(p_0,p)] + p[2\psi_{a0}(p_0,p)^2 + 2\sqrt{2}\psi_{a0}(p_0,p)\psi_{a2}(p_0,p) + \psi_{a2}(p_0,p)^2 - 8\psi_{t0}(p_0,p)^2 \\ &- 8\sqrt{2}\psi_{t0}(p_0,p)\psi_{t2}(p_0,p) - 4\psi_{t2}(p_0,p)^2 - 12\psi_{t1}^0(p_0,p)^2 + 3\psi_{v1}(p_0,p)^2] \Bigg\}, \end{aligned} \tag{A6}$$

$$\begin{aligned} \vec{f}_3^{N/D}(p) = \Bigg\{ &p\left(\frac{-8\psi_{p1}(p_0,p)\psi_{t0}(p_0,p)}{\sqrt{3}} - 4\sqrt{\frac{2}{3}}\psi_{p1}(p_0,p)\psi_{t2}(p_0,p) - 2\sqrt{\frac{2}{3}}\psi_{a0}(p_0,p)\psi_{v1}(p_0,p) \right. \\ &\left. - \frac{8\psi_{a2}(p_0,p)\psi_{v1}(p_0,p)}{\sqrt{3}} \right) + m[4\sqrt{2}\psi_{a2}(p_0,p)\psi_{t0}(p_0,p) + 4\sqrt{2}\psi_{a0}(p_0,p)\psi_{t2}(p_0,p) + 8\psi_{a2}(p_0,p)\psi_{t2}(p_0,p) \\ &+ 4\sqrt{2}\psi_{a1}^0(p_0,p)\psi_{t1}^0(p_0,p) - 2\sqrt{2}\psi_{p1}(p_0,p)\psi_{v1}(p_0,p)] + \left(\frac{1}{2}M_d - p_0 \right)[-2\sqrt{2}\psi_{a0}(p_0,p)\psi_{a2}(p_0,p) \\ &- 2\psi_{a2}(p_0,p)^2 - 8\sqrt{2}\psi_{t0}(p_0,p)\psi_{t2}(p_0,p) - 8\psi_{t2}(p_0,p)^2 - 8\psi_{t1}^0(p_0,p)^2 - 2\psi_{v1}(p_0,p)^2] \Bigg\} P_2[\cos(\theta)] \\ &+ p\left(\frac{8\psi_{p1}(p_0,p)\psi_{t0}(p_0,p)}{\sqrt{3}} + 4\sqrt{\frac{2}{3}}\psi_{p1}(p_0,p)\psi_{t2}(p_0,p) - 4\sqrt{\frac{2}{3}}\psi_{a0}(p_0,p)\psi_{v1}(p_0,p) + \frac{2\psi_{a2}(p_0,p)\psi_{v1}(p_0,p)}{\sqrt{3}} \right) \\ &+ m[8\psi_{a0}(p_0,p)\psi_{t0}(p_0,p) - 4\psi_{a2}(p_0,p)\psi_{t2}(p_0,p) - 4\sqrt{2}\psi_{a1}^0(p_0,p)\psi_{t1}^0(p_0,p) + 2\sqrt{2}\psi_{p1}(p_0,p)\psi_{v1}(p_0,p)] \end{aligned}$$

$$+\left(\frac{1}{2}M_d-p_0\right)[-2\psi_{a0}(p_0,p)^2+\psi_{a2}(p_0,p)^2-8\psi_{t0}(p_0,p)^2+4\psi_{t2}(p_0,p)^2-4\psi^0_{t1}(p_0,p)^2-\psi_{v1}(p_0,p)^2], \tag{A7}$$

$$\Delta f_0^{N/D}(p)=P_2[\cos(\theta)]\Big\{m[-12\sqrt{2}\psi_{a2}(p_0,p)\psi_{t0}(p_0,p)-12\sqrt{2}\psi_{a0}(p_0,p)\psi_{t2}(p_0,p)+12\psi_{a2}(p_0,p)\psi_{t2}(p_0,p)]$$
$$+p[8\sqrt{3}\psi_{p1}(p_0,p)\psi_{t0}(p_0,p)-8\sqrt{6}\psi_{p1}(p_0,p)\psi_{t2}(p_0,p)+2\sqrt{6}\psi_{a0}(p_0,p)\psi_{v1}(p_0,p)$$
$$+2\sqrt{3}\psi_{a2}(p_0,p)\psi_{v1}(p_0,p)]+\left(\frac{1}{2}M_d-p_0\right)[-6\psi^0_{a1}(p_0,p)^2+6\sqrt{2}\psi_{a0}(p_0,p)\psi_{a2}(p_0,p)-3\psi_{a2}(p_0,p)^2$$
$$-6\psi_{p1}(p_0,p)^2+24\sqrt{2}\psi_{t0}(p_0,p)\psi_{t2}(p_0,p)-12\psi_{t2}(p_0,p)^2+12\psi^0_{t1}(p_0,p)^2+3\psi_{v1}(p_0,p)^2]\Big\}, \tag{A8}$$

$$\Delta f_3^{N/D}(p)=\cos(\theta)\Big\{p[-4\psi_{a0}(p_0,p)^2+2\sqrt{2}\psi_{a0}(p_0,p)\psi_{a2}(p_0,p)+4\psi_{a2}(p_0,p)^2+16\psi_{t0}(p_0,p)^2-8\sqrt{2}\psi_{t0}(p_0,p)\psi_{t2}(p_0,p)$$
$$-16\psi_{t2}(p_0,p)^2]+\left(\frac{1}{2}M_d-p_0\right)[-8\sqrt{3}\psi_{p1}(p_0,p)\psi_{t0}(p_0,p)-4\sqrt{6}\psi_{p1}(p_0,p)\psi_{t2}(p_0,p)$$
$$-2\sqrt{6}\psi_{a0}(p_0,p)\psi_{v1}(p_0,p)+4\sqrt{3}\psi_{a2}(p_0,p)\psi_{v1}(p_0,p)]+m[4\sqrt{3}\psi_{a0}(p_0,p)\psi_{p1}(p_0,p)$$
$$+2\sqrt{6}\psi_{a2}(p_0,p)\psi_{p1}(p_0,p)+4\sqrt{6}\psi_{t0}(p_0,p)\psi_{v1}(p_0,p)-8\sqrt{3}\psi_{t2}(p_0,p)\psi_{v1}(p_0,p)]$$
$$+P_2[\cos(\theta)]\left[\left(\frac{1}{2}M_d-p_0\right)[12\sqrt{6}\psi_{p1}(p_0,p)\psi_{t2}(p_0,p)-6\sqrt{3}\psi_{a2}(p_0,p)\psi_{v1}(p_0,p)\right]$$
$$+m[-6\sqrt{6}\psi_{a2}(p_0,p)\psi_{p1}(p_0,p)$$
$$+12\sqrt{3}\psi_{t2}(p_0,p)\psi_{v1}(p_0,p)\Big]+p[-6\psi^0_{a1}(p_0,p)^2-9\psi_{a2}(p_0,p)^2+6\psi_{p1}(p_0,p)^2+36\psi_{t2}(p_0,p)^2+12\psi^0_{t1}(p_0,p)^2$$
$$-3\psi_{v1}(p_0,p)^2] \tag{A9}$$

APPENDIX B: HADRONIC TENSOR FOR THE DEUTERON PROJECTORS

The parametrization of the hadronic tensor for the deuteron utilized in the present paper is given by Eq. (3.1). It has both symmetric $\{\cdots\}$, and antisymmetric $[\cdots]$ parts with respect to permutation of its indices

$$W^D_{\mu\nu}=W^D_{\{\mu\nu\}}+W^D_{[\mu\nu]}. \tag{B1}$$

Three physical vectors are used in this parametrization: (1) P_D the deuteron momentum. In the rest frame of the deuteron $P_D=(M_D,\mathbf{0})$, (2) q the momentum transfer in deep inelastic scattering. With proper choice of the orientation of the coordinate system $q=(\nu,0,0,-\sqrt{\nu^2+Q^2})$. In the deep inelastic limit, when $Q^2/\nu^2\to 0$, $pq=\nu(p_0+p_3)$, and (3) $S_D(M)$ is the total angular momentum of the deuteron, i.e., spin of the deuteron as an elementary particle:

$$S^\alpha_D(M)=-\frac{i}{M_D}\epsilon^{\alpha\beta\gamma\delta}E^*_\beta(M)E_\gamma(M)P_{D\delta}, \tag{B2}$$

$$E(M)=\begin{cases}\dfrac{1}{\sqrt{2}}(0,-1,-i,0), & M=1,\\ (0,0,0,1), & M=0,\\ \dfrac{1}{\sqrt{2}}(0,1,-i,0), & M=-1.\end{cases} \tag{B3}$$

The symmetric part of the hadronic tensor $W^D_{\{\mu\nu\}}$ contains terms proportional to two tensor structures:

$$T^{(1)}_{\mu\nu}=-g_{\mu\nu}+\frac{q_\mu q_\nu}{q^2}, \tag{B4}$$

$$T^{(2)}_{\mu\nu}=\left(P_{D\mu}-q_\mu\frac{P_Dq}{q^2}\right)\left(P_{D\nu}-q_\nu\frac{P_Dq}{q^2}\right)\frac{1}{P_Dq}. \tag{B5}$$

Because of the conservation of the electromagnetic current, the contraction of the hadronic tensor with q_μ with any index is zero. For this reason only $P_{D\mu}P_{D\nu}$ and $g_{\mu\nu}$ are available to construct the projection operators to extract the structure functions F^D_1 and F^D_2 from the hadronic tensor. We introduce the coefficients

$$C_1 \equiv g^{\mu\nu} T^{(1)}_{\mu\nu}, \quad C_2 \equiv g^{\mu\nu} T^{(2)}_{\mu\nu},$$

$$C_3 \equiv \frac{P^\mu_D P^\nu_D}{P^2_D} T^{(1)}_{\mu\nu}, \quad C_4 \equiv \frac{P^\mu_D P^\nu_D}{P^2_D} T^{(2)}_{\mu\nu}, \tag{B6}$$

$$D_C \equiv C_1 C_4 - C_2 C_3, \tag{B7}$$

$$A_1 \equiv g^{\mu\nu} W^D_{\mu\nu}, \quad A_2 \equiv \frac{P^\mu_D P^\nu_D}{P^2_D} W^D_{\mu\nu}. \tag{B8}$$

Then the structure functions are recovered by

$$F^D_1 = \frac{A_1 C_4 - A_2 C_2}{D_C}, \tag{B9}$$

$$F^D_2 = \frac{A_2 C_1 - A_1 C_3}{D_C}. \tag{B10}$$

In the general case the antisymmetric part of the hadronic tensor of the deuteron $W^D_{[\mu\nu]}$ has the form

$$W^D_{[\mu\nu]} = \frac{i M_D}{P_D q} \epsilon_{\mu\nu\alpha\beta} q^\alpha \Big\{ S^\beta_D(M) [g^D_1(x_D, Q^2) + g^D_2(x_D, Q^2)] - P^\beta_D \frac{(S_D(M) q)}{P_D q} g^D_2(x_D, Q^2) \Big\}, \tag{B11}$$

where the second structure function g^D_2 vanishes in the deep inelastic limit $\nu \to \infty$, $Q^2 \to \infty$, $Q^2/\nu \to$ const. We do not discuss this structure function in the present paper. To obtain the spin-dependent structure function g^D_1 we construct antisymmetric projectors. The two following projectors are equivalent for our purpose:

$$R^{(1)}_{\mu\nu} \equiv i \epsilon_{\mu\nu\alpha\beta} q^\alpha S^\beta_D(M), \tag{B12}$$

$$R^{(2)}_{\mu\nu} \equiv \frac{i [S_D(M) q]}{P_D q} \epsilon_{\mu\nu\alpha\beta} q^\alpha P^\beta_D. \tag{B13}$$

So it is interesting that in the limit $Q^2/\nu^2 \to 0$

$$g^D_1 = \frac{R^{(1)\mu\nu} W^D_{\mu\nu}}{2\nu} = \frac{R^{(2)\mu\nu} W^D_{\mu\nu}}{2\nu}. \tag{B14}$$

[1] A.Yu. Umnikov and F.C. Khanna, Phys. Rev. C **49**, 2311 (1994); Mod. Phys. Lett. A **10**, 91 (1995).

[2] A.Yu. Umnikov, L.P. Kaptari, K.Yu. Kazakov, and F. Khanna, Phys. Lett. B **334**, 163 (1994).

[3] F.C. Khanna, L.P. Kaptari, and A.Yu. Umnikov, Czech. J. Phys. **45**, 363 (1995).

[4] A.Yu. Umnikov, L.P. Kaptari, K.Yu. Kazakov, and F.C. Khanna, in Proceedings of the 14th International Conference on Few-Body Problems in Physics, Williamsburg, Virginia, 1994, edited by F. Gross, AIP Conf. Proc. No. 334 (AIP, New York, (1995), p. 749; in Proceedings of the 11th International Symposium on High-Energy Spin Physics and 8th International Symposium on Polarization Phenomena in Nuclear Physics, Bloomington, Indiana, 1994, edited by E. J. Stephenson and S. E. Vigdor, AIP Conf Proc. No. 339 (AIP, New York, 1995), p. 79.

[5] L.I. Frankfurt and M.S. Strikman, Phys. Lett. **64B**, 433 (1976); **65B**, 51 (1976); **76B**, 333 (1978).

[6] P.V. Landshoff and J.C. Polkinghorne, Phys. Rev. D **18**, 153 (1978).

[7] D. Kusno and M.J. Moravcsik, Phys. Rev. D **20**, 2734 (1979).

[8] P.J. Mulders, A.W. Schreiber, and H. Meyer, Nucl. Phys. **A549**, 498 (1992).

[9] W. Melnitchouk, A.W. Schreiber, and A.W. Thomas, Phys. Rev. D **49**, 1183 (1994).

[10] W. Melnitchouk, A.W. Schreiber, and A.W. Thomas, Phys. Lett. B **335**, 11 (1995).

[11] W. Melnitchouk, G. Piller, and A.W. Thomas, Phys. Lett. B **346**, 165 (1995).

[12] S. Kulagin, W. Melnitchouk, G. Piller, and W. Weise, Phys. Rev. C **52**, 932 (1995).

[13] M. Braun and M. Tokarev, Phys. Lett. B **320**, 381 (1994).

[14] F. Lev, Nucl. Phys. **A606**, 459 (1996); e-print hep-ph/9507421.

[15] S.V. Akulinichev, S.A. Kulagin, and G.M. Vagradov, Phys. Lett. **158B**, 485 (1985); JETP Lett. **42**, 127 (1985).

[16] B.L. Birbrair, E.M. Levin, and A.G. Shuvaev, Nucl. Phys. **A496**, 704 (1989).

[17] L.P. Kaptari, A.Yu. Umnikov, and B. Kämpfer, Phys. Rev. D **47**, 3804 (1993); L.P. Kaptari, K.Yu. Kazakov, and A.Yu. Umnikov, Phys. Lett. B **293**, 219 (1992).

[18] M. Lacombe, B. Loiseau, J.M. Richard, R. Vinh Mau, J. Côte, P. Pirès, and R. de Tourreil , Phys. Rev. C **21**, 861 (1980).

[19] R. Machleidt, K. Holinde, and Ch. Elster, Phys. Rep. **149**, 1 (1987).

[20] W.W. Buck and F. Gross, Phys. Rev. C **20**, 2361 (1979).

[21] M.J. Zuilhof and J.A. Tjon, Phys. Rev. C **22**, 2369 (1980).

[22] F. Gross, J.W. Van Orden, and K. Holinde, Phys. Rev. C **45**, 2094 (1992).

[23] See, e.g. M.C. Birse and B. Krippa, Phys. Lett. B **373**, 9 (1996), and references therein; H. Shiomi and T. Hatsuda, Nucl. Phys. **A594**, 294 (1995), and references therein.

[24] See, e.g., C.A. de Rocha and M.R. Robilotta, Phys. Rev. C **52**, 531 (1995), and references therein; **4**, 1818 (1994), and references therein; C. Ordonez, L. Ray, and U. van Kolck, *ibid.* **53**, 2086 (1996;), and references therein.

[25] J. Fleischer and J.A. Tjon, Nucl. Phys. **B84**, 375 (1975); Phys. Rev. D **15**, 2537 (1977).

[26] F. Gross, in *Electromagnetic Studies of the Deuteron*, Proceedings of the 9th Amsterdam Miniconference, 1996, NIKHEF, Amsterdam, 1996 (unpublished), p. 1.

[27] R.A. Arndt, I.I. Strakovsky, and R.L. Workman, Phys. Rev. C **50**, 2731 (1994).

[28] A.Yu. Umnikov and F.C. Khanna, Int. J. Mod. Phys. A **10**, 3935 (1996).
[29] A. Umnikov, Z. Phys. A **357**, 333 (1997).
[30] L.P. Kaptari, A.Yu. Umnikov, S. Bondarenko, K. Kazakov, F.C. Khanna, and B. Kämpfer, Phys. Rev. C **54**, 986 (1996).
[31] E. Hummel and J.A. Tjon, Phys. Rev. C **49**, 21 (1994).
[32] J.W. Van Orden, E. Devine, and F. Gross, Phys. Rev. Lett. **75**, 4369 (1995).
[33] L. Mathelitsch *et al.*, in *Electromagnetic Studies of the Deuteron* [26], p. 41.
[34] K.G. Wilson, Phys. Rev. **179**, 1499 (1969): R.A. Brandt and G. Preparata, Nucl. Phys. **B27**, 541 (1971): W. Zimmermann, Ann. Phys. (N.Y.) **77**, 570 (1973).
[35] C. Ciofi degli Atti, L.P. Kaptari, K. Yu. Kazakov, S. Scopetta, and A. Yu. Umnikov, Phys. Rev. C **51**, 52 (1995).
[36] F. Gross and S. Liuti, Phys. Rev. C **45**, 1374 (1992).
[37] A.V. Efremov and O.V. Teryaev, Sov. J. Nucl. Phys. **36**, 557 (1982).
[38] L.I. Frankfurt and M.S. Strikman, Phys. Rep. **76**, 216 (1981): Nucl. Phys. **A405**, 557 (1983).
[39] R.L. Jaffe and A. Manohar, Nucl. Phys. **B321**, 343 (1989); P. Hoodbhoy, R.L. Jaffe, and A. Manohar, *ibid.* **B312**, 571 (1989).
[40] L.P. Kaptari and A. Yu. Umnikov, Z. Phys. A **341**, 353 (1992).
[41] R.L. Jaffe, in *Relativistic Dynamics and Quark-Nuclear Physics*, edited by M.B. Johnson and A. Picklesimer (Wiley, New York, 1987), p. 537.
[42] A. Yu. Umnikov, L.P. Kaptari, and F. Khanna, Phys. Rev. C **53**, 377 (1996).
[43] S. Kulagin, Nucl. Phys. **A500**, 653 (1989).
[44] L.S. Celenza, C.M. Shakin, and W. Koepf, Phys. Rev. C **42**, 1989 (1990).
[45] L.P. Kaptari and A.Yu. Umnikov, Phys. Lett. B **259**, 155 (1991).
[46] A. Schäfer, Phys. Lett. B **208**, 175 (1988).
[47] S. Wolfram, MATHEMATICA (Addison-Wesley, Reading, MA, 1993).